
# Working towards all the geophysics - but backwards.

Rowan Cockett, Seogi Kang & SimPEG Team
July 12, 2016



Geophysical Inversion Facility
University of British Columbia

some of

# Working towards all the geophysics - but backwards.

Rowan Cockett, Seogi Kang & SimPEG Team

July 12, 2016

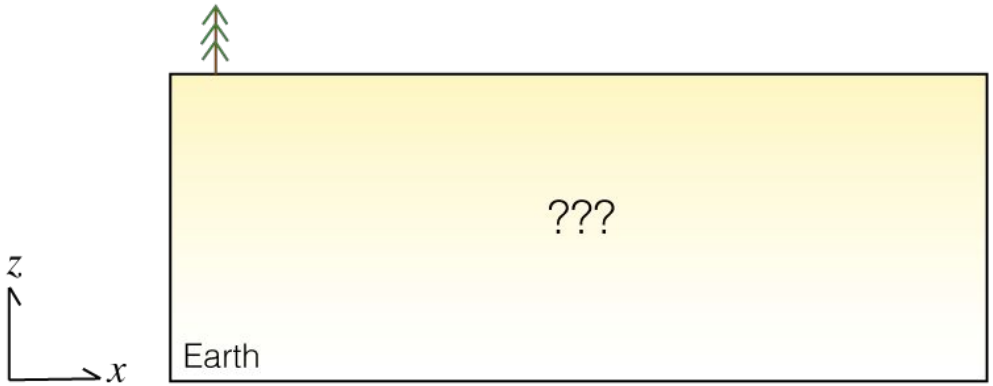


The Subsurface

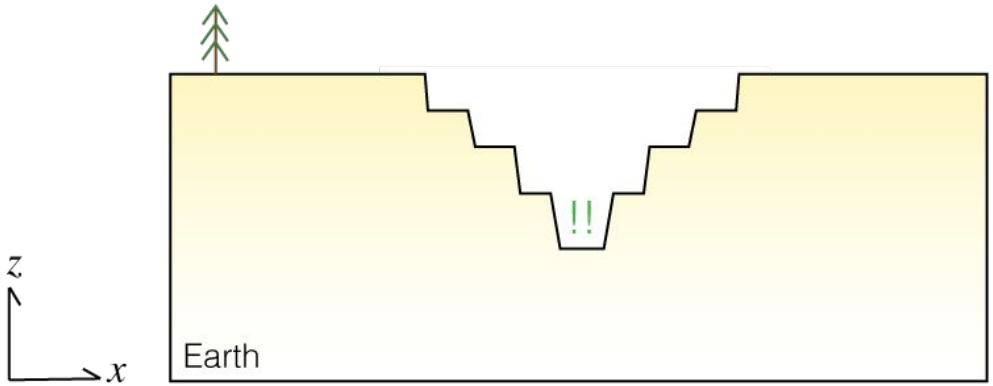


Option 1: Dig it up?

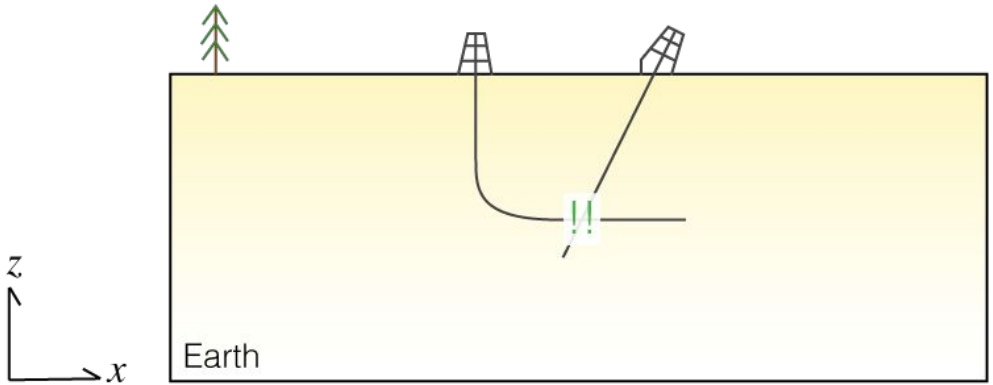


Option 2: Drill it?

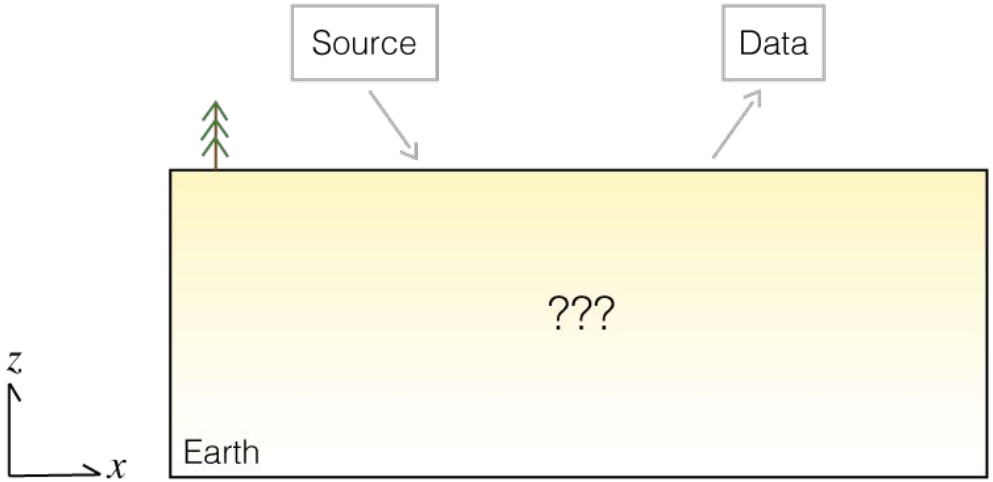


Option 3: Use geophysics!

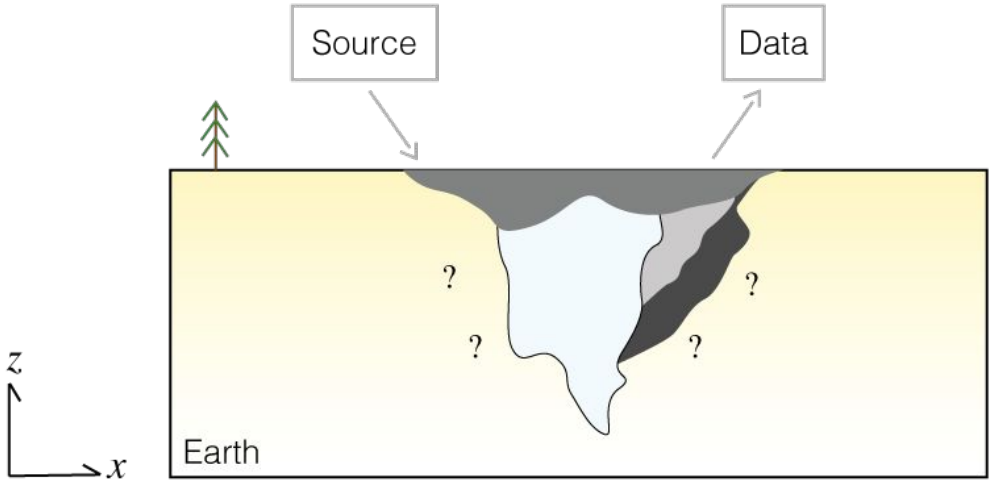


Physical properties

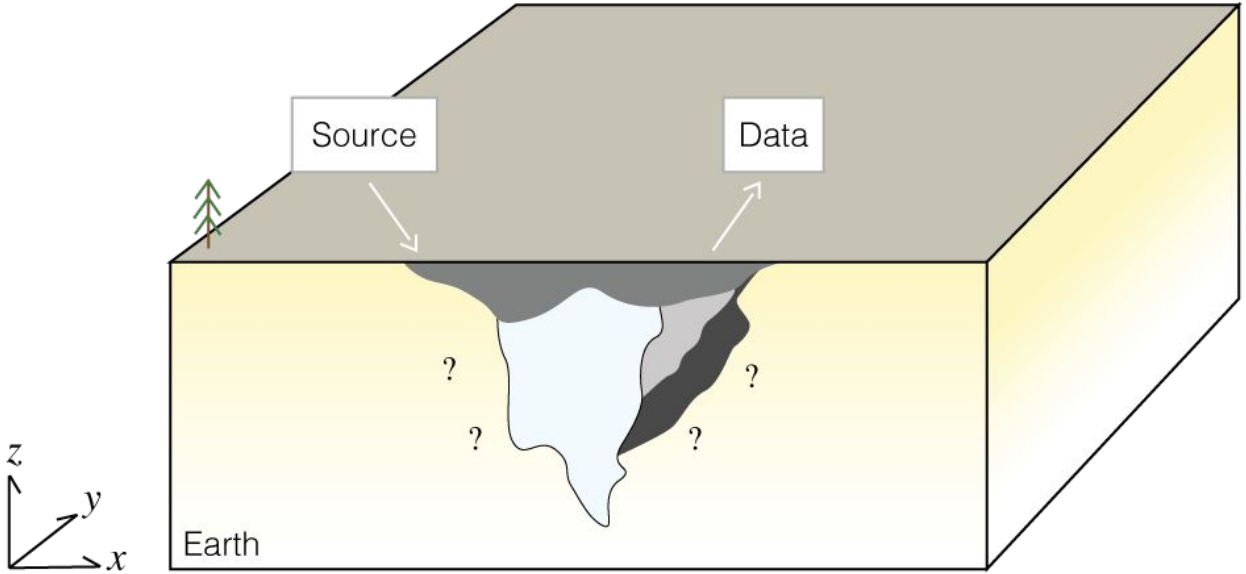


The world is 3D

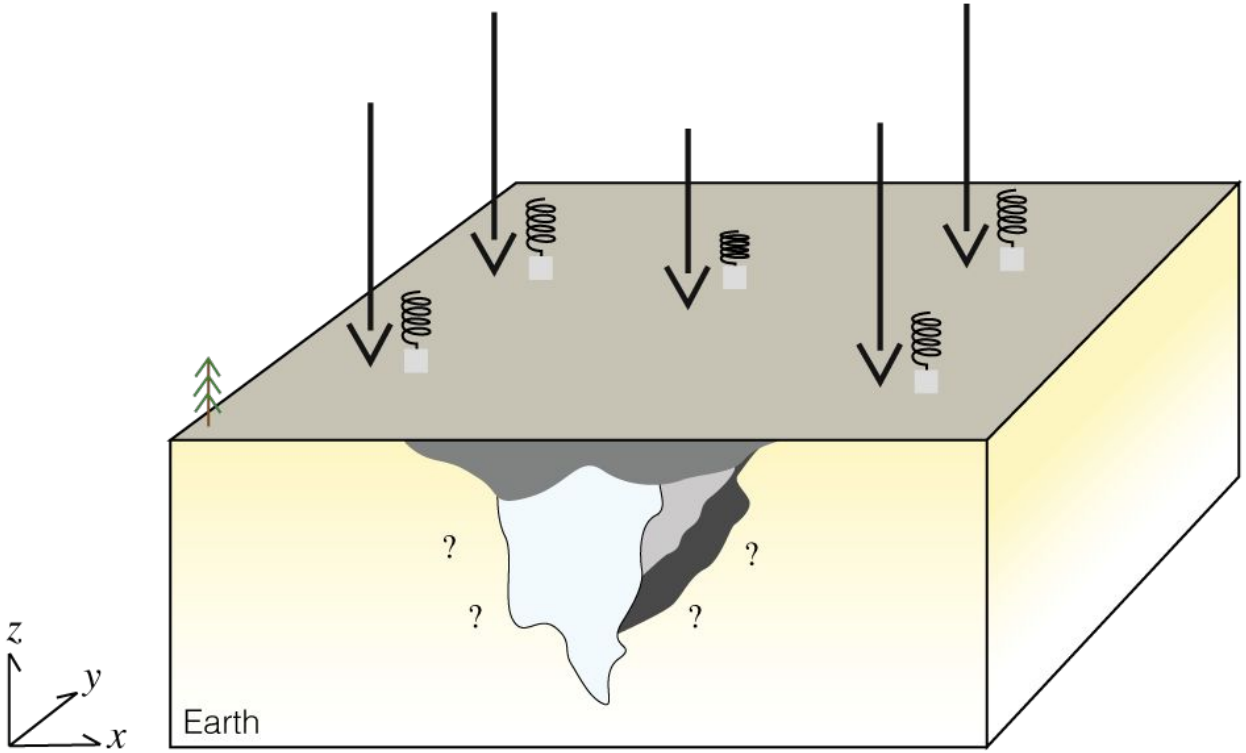


Gravity

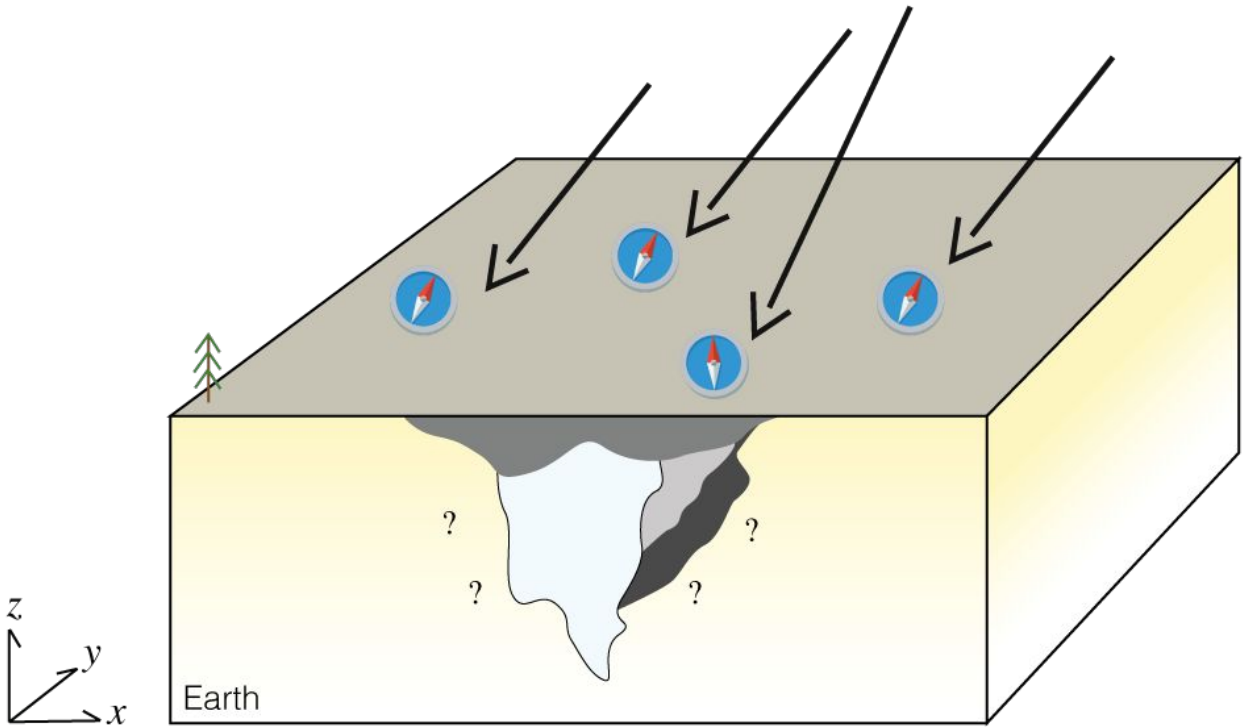
z
y
x
Earth
?
?
?
?

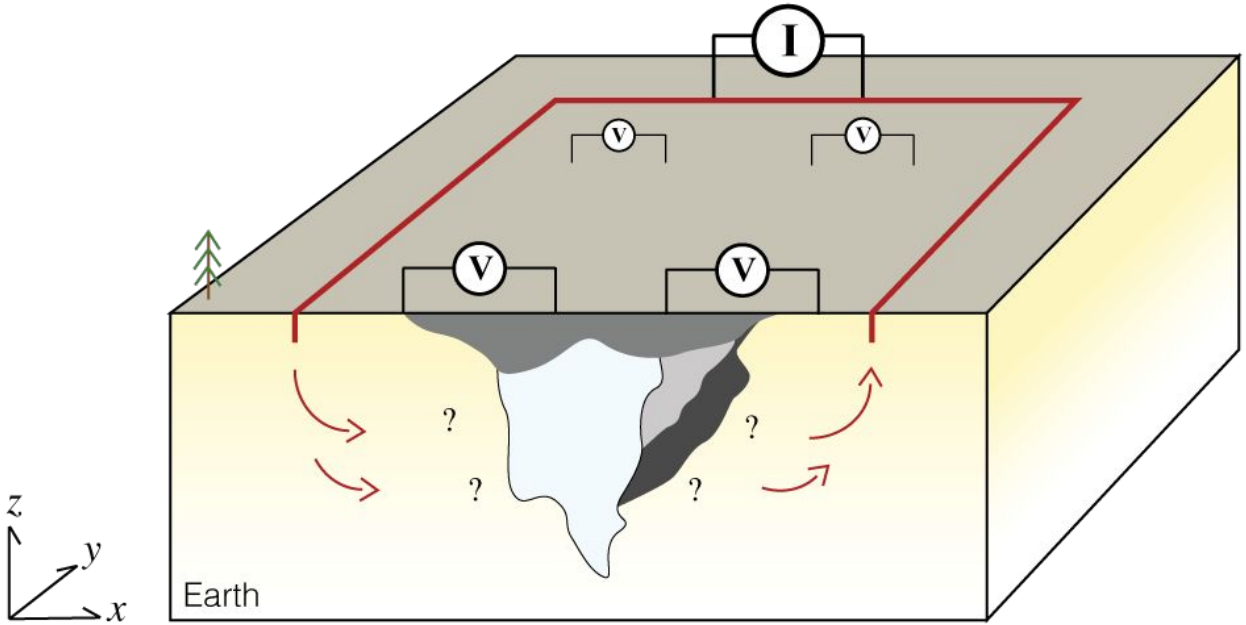


Direct current resistivity

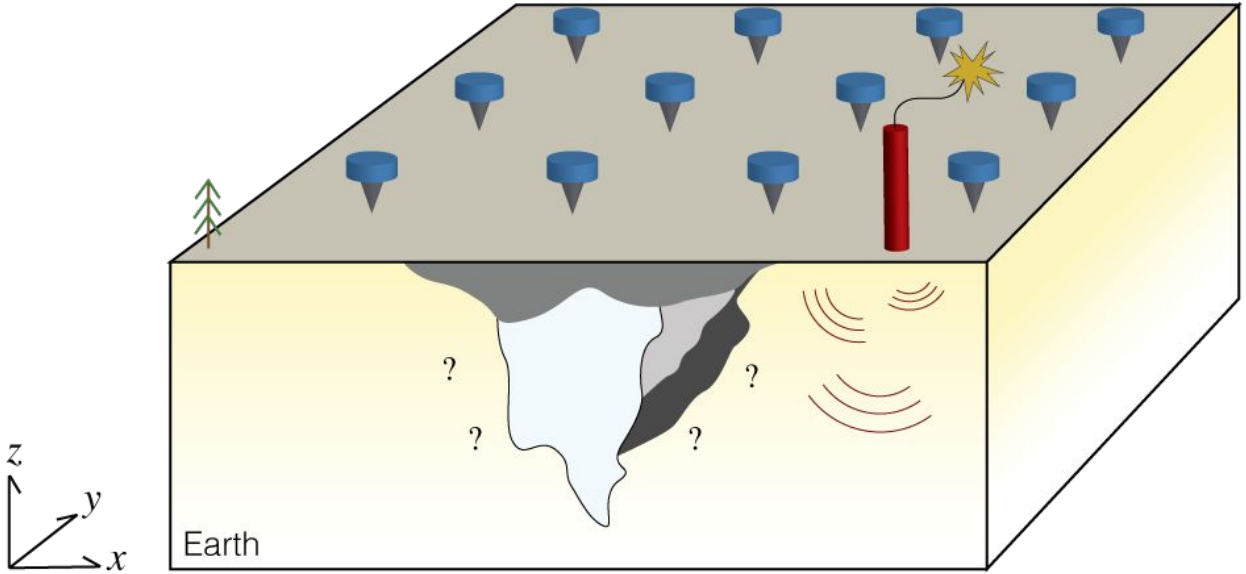


Seismic

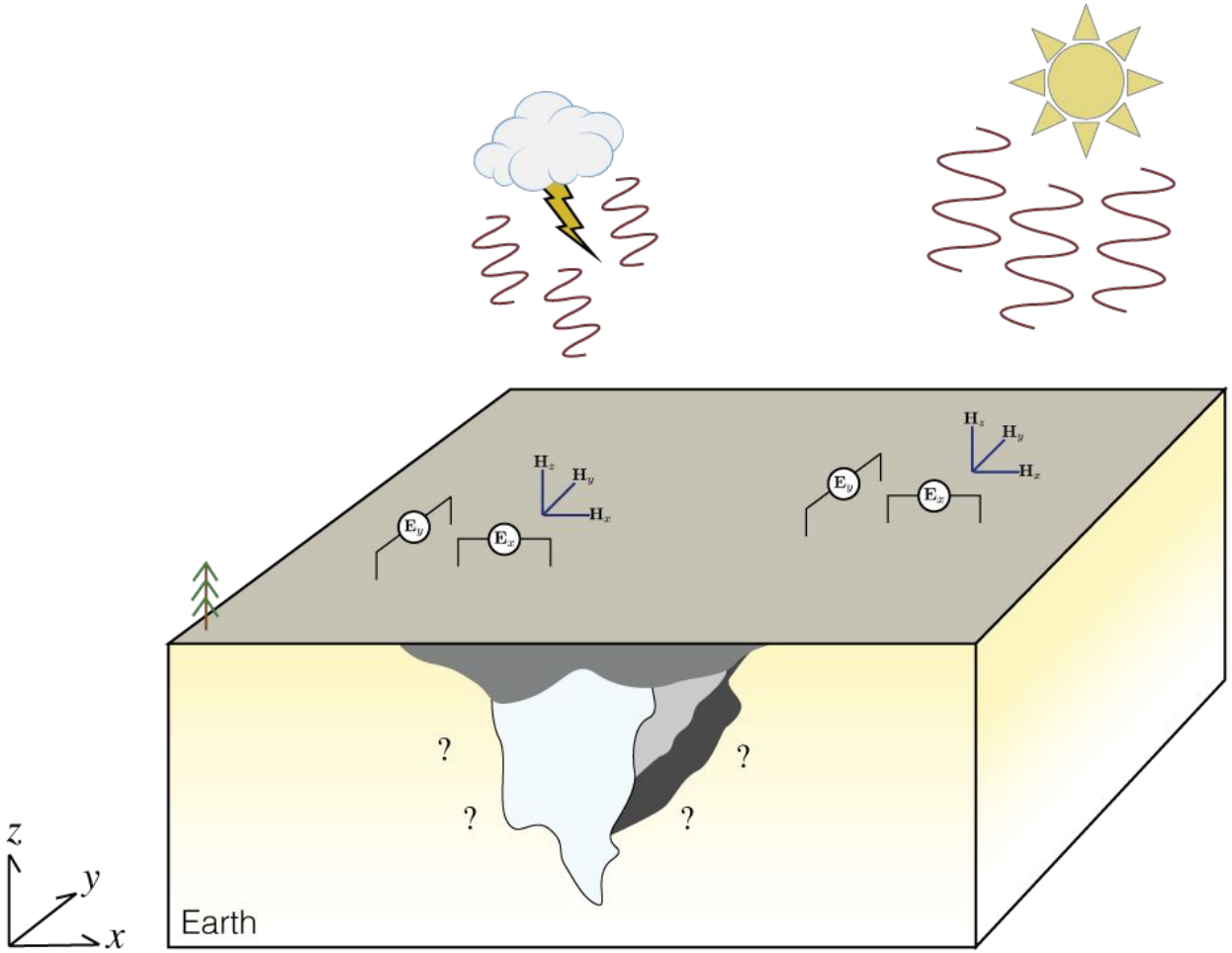


Magnetotellurics

Predict & Decide

## Hydrogeology

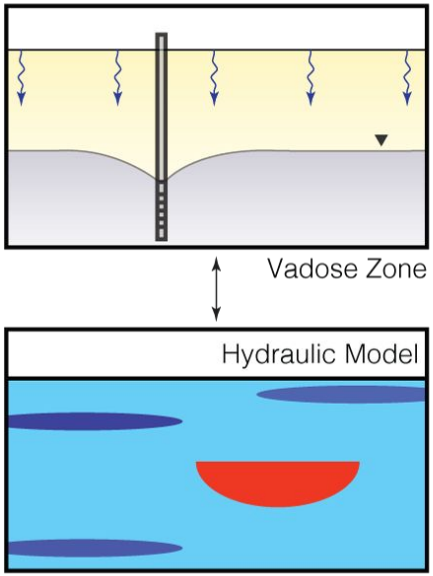


## Geophysics

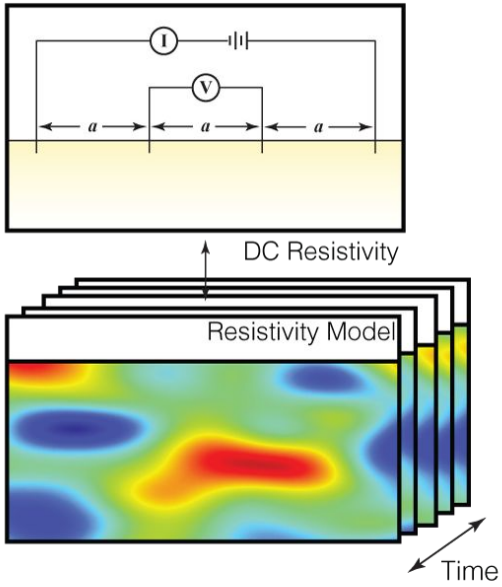


## Geology

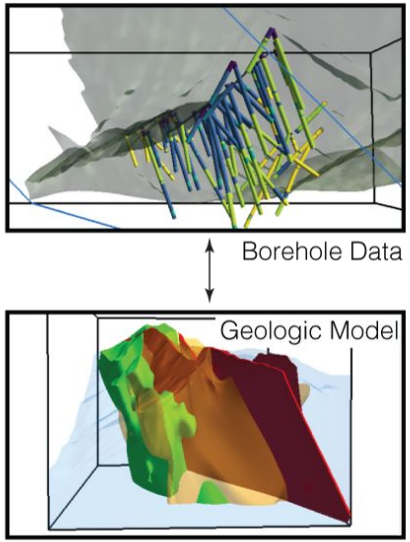

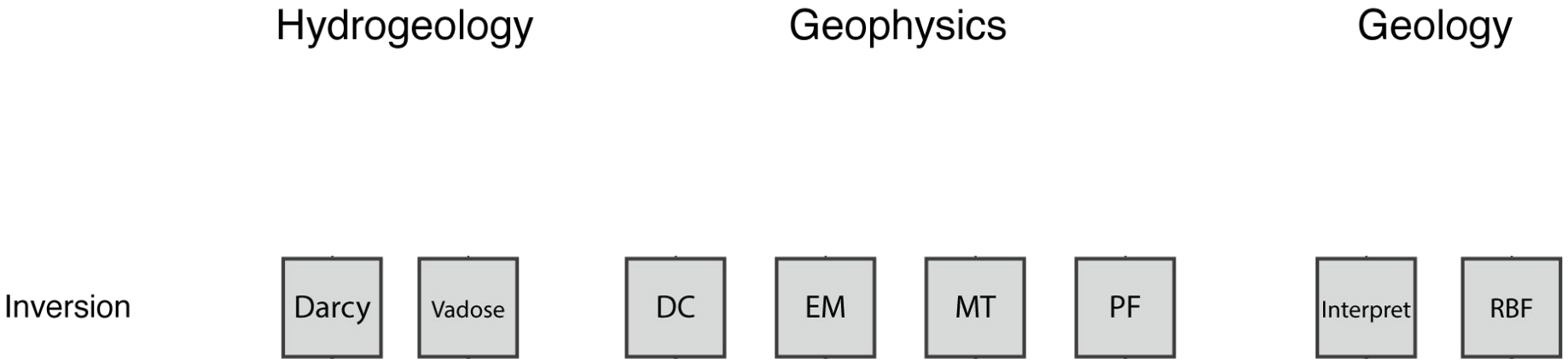
Hydrogeology
Geophysics
Geology
Inversion
Darcy
Vadose
DC
EM
MT
PF
Interpret
RBF

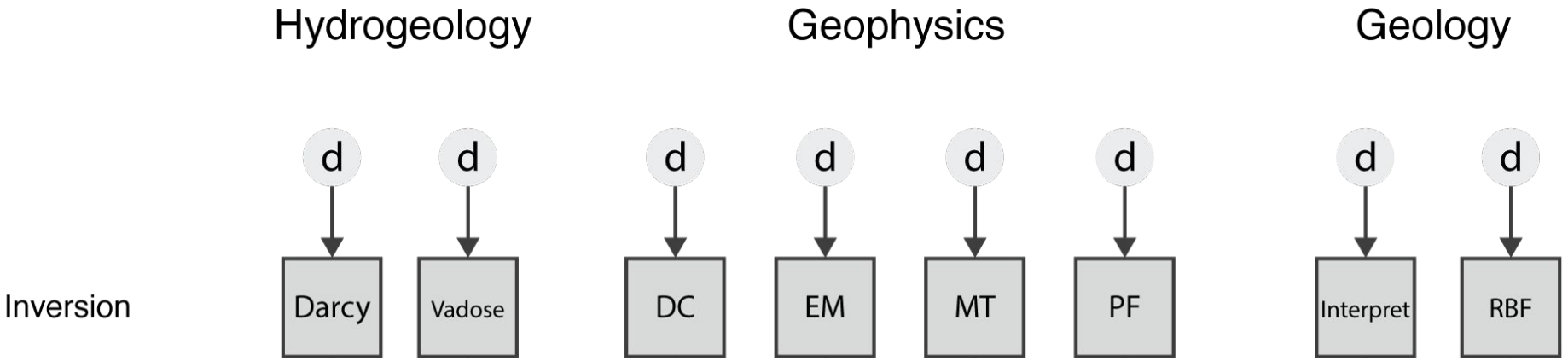
Hydrogeology
Geophysics
Geology
Inversion
d
d
d
d
d
d
d
d
Darcy
Vadose
DC
EM
MT
PF
Interpret
RBF

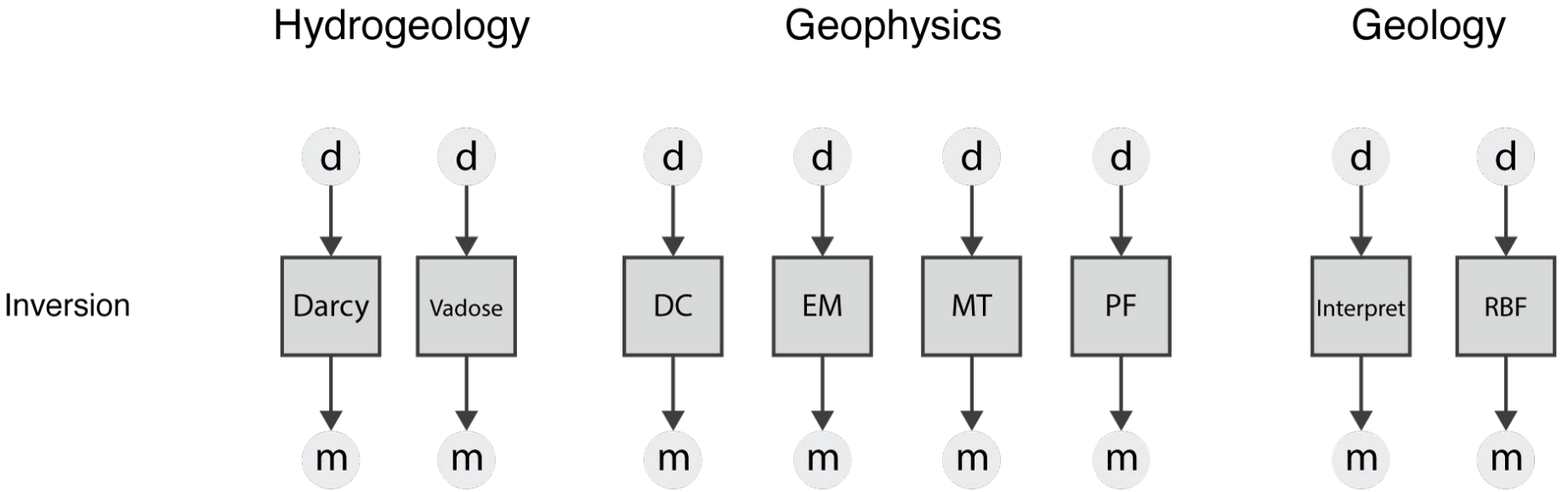
Hydrogeology
Geophysics
Geology
Inversion
d
d
d
d
d
d
d
d
Darcy
Vadose
DC
EM
MT
PF
Interpret
RBF
m
m
m
m
m
m
m
m

Inversion

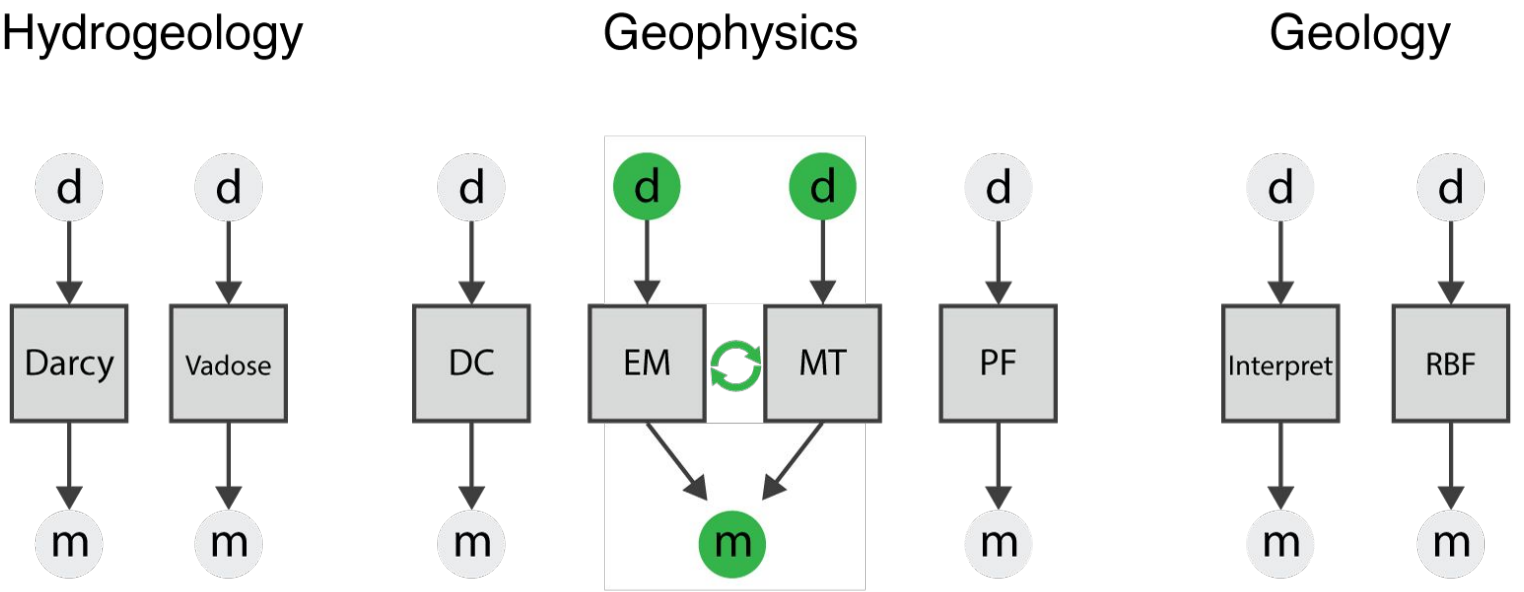
Hydrogeology
Geophysics
Geology
d
d
Darcy
Vadose
m
m
d
DC
m
d
d
EM
MT
m
d
PF
m
d
d
Interpret
RBF
m
m

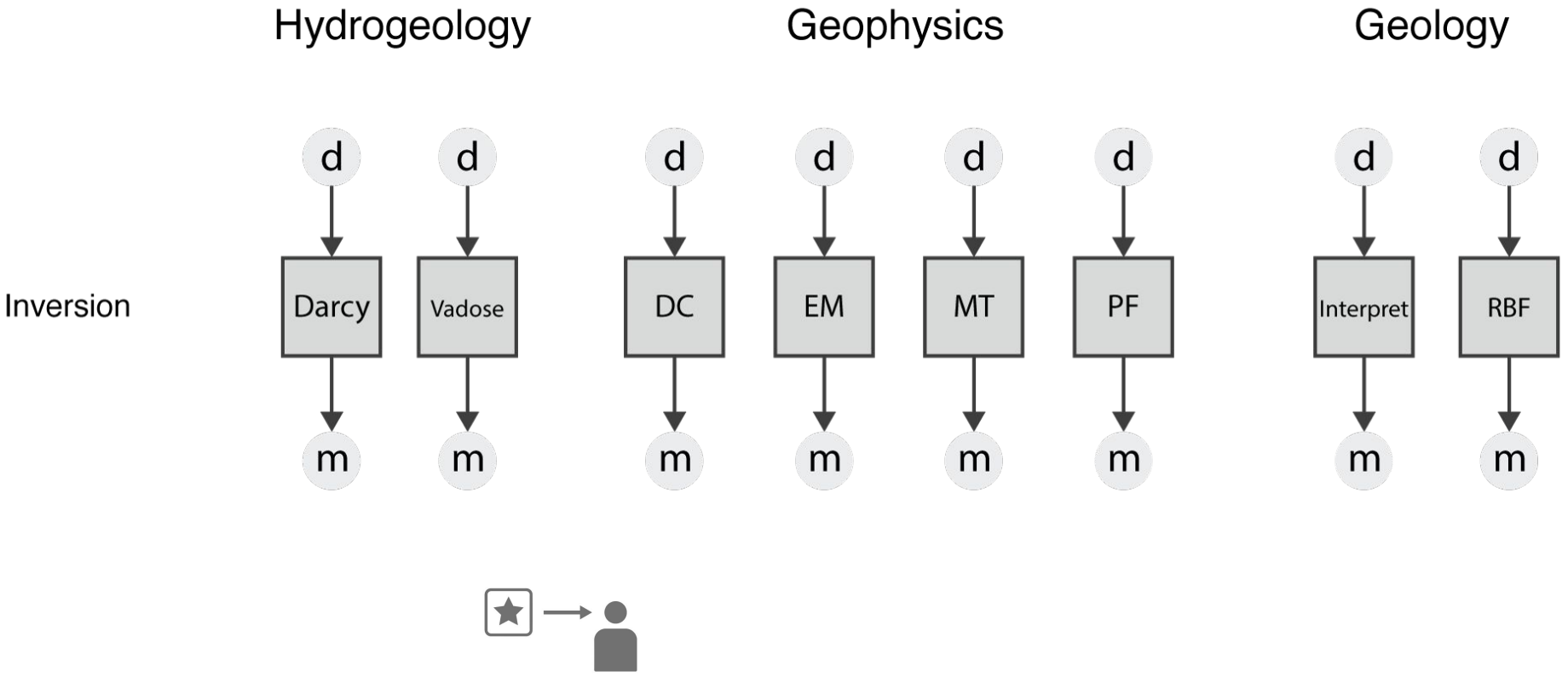
Hydrogeology
Geophysics
Geology
Inversion
d
d
d
d
d
d
d
d
Darcy
Vadose
DC
EM
MT
PF
Interpret
RBF
m
m
m
m
m
m
m
m

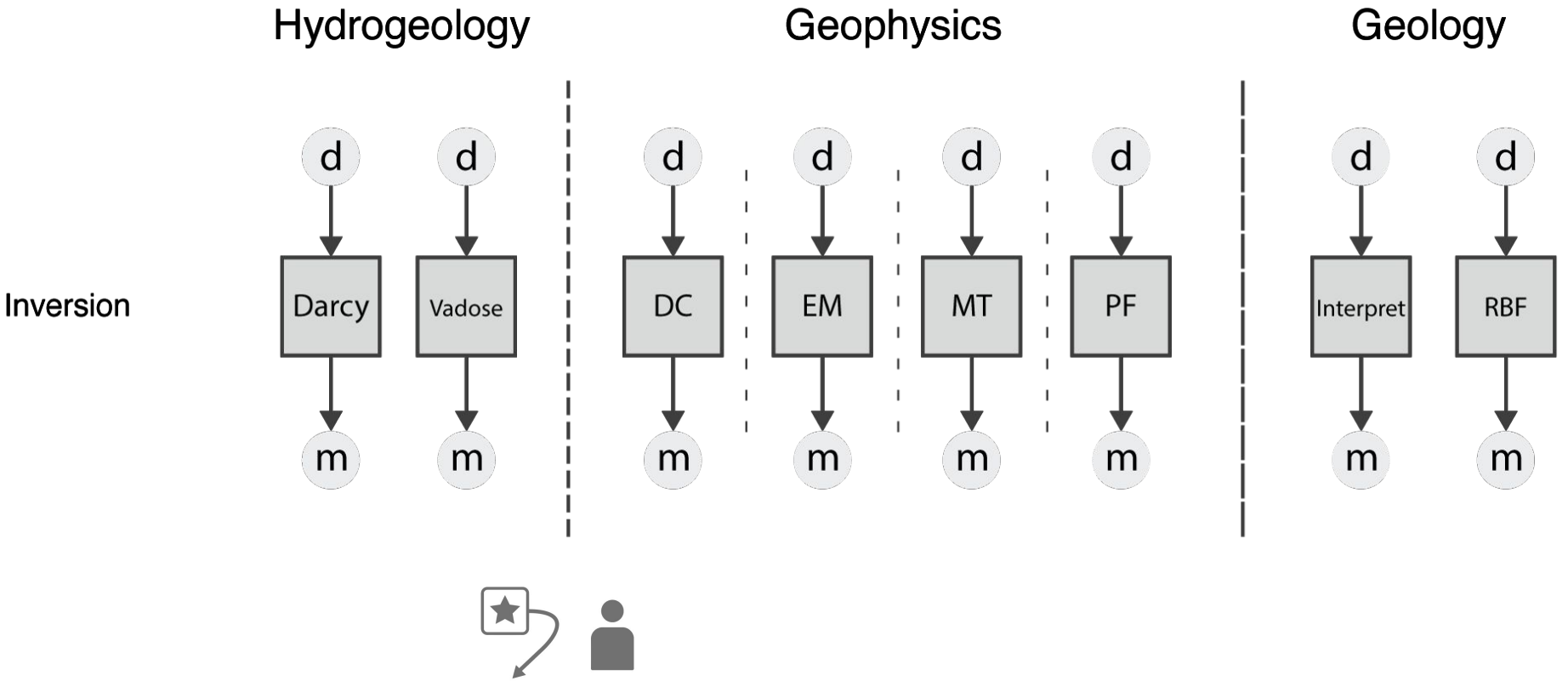
Hydrogeology
Geophysics
Geology
Inversion
d
d
d
d
d
d
d
d
Darcy
Vadose
DC
EM
MT
PF
Interpret
RBF
m
m
m
m
m
m
m
m

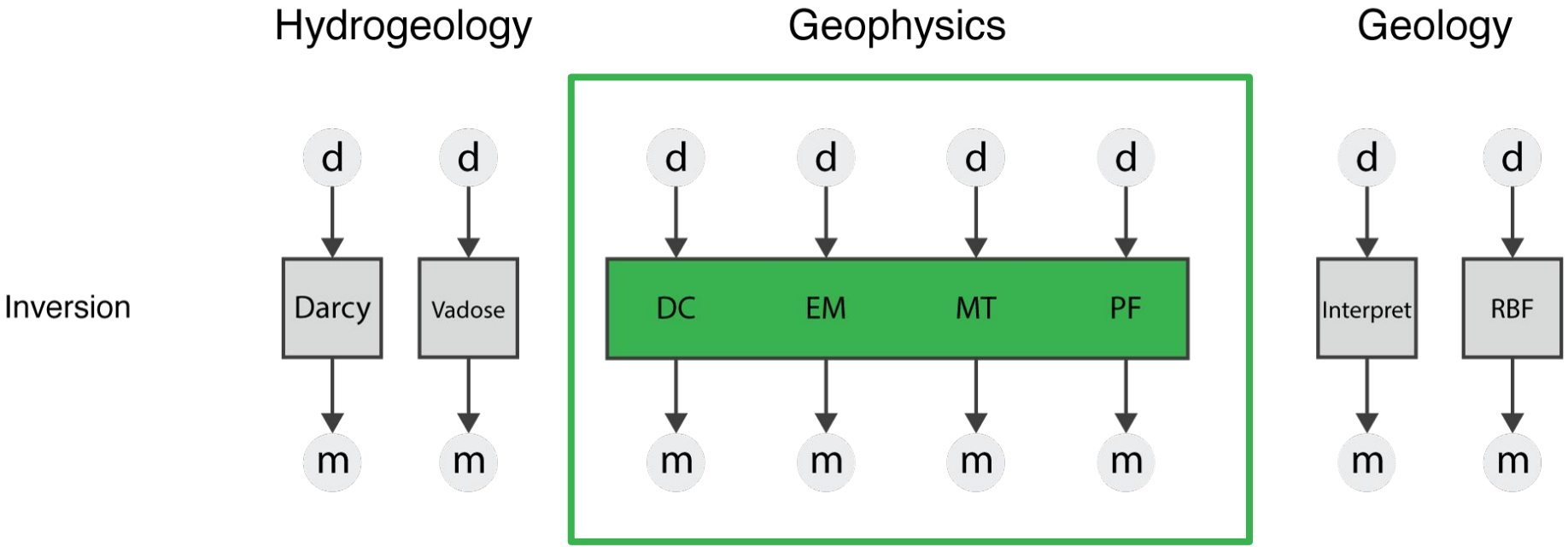
Hydrogeology
Geophysics
Geology
Inversion
d
d
d
d
d
d
d
d
d
Darcy
Vadose
DC
EM
MT
PF
Interpret
RBF
m
m
m
m
m
m
m
m
m

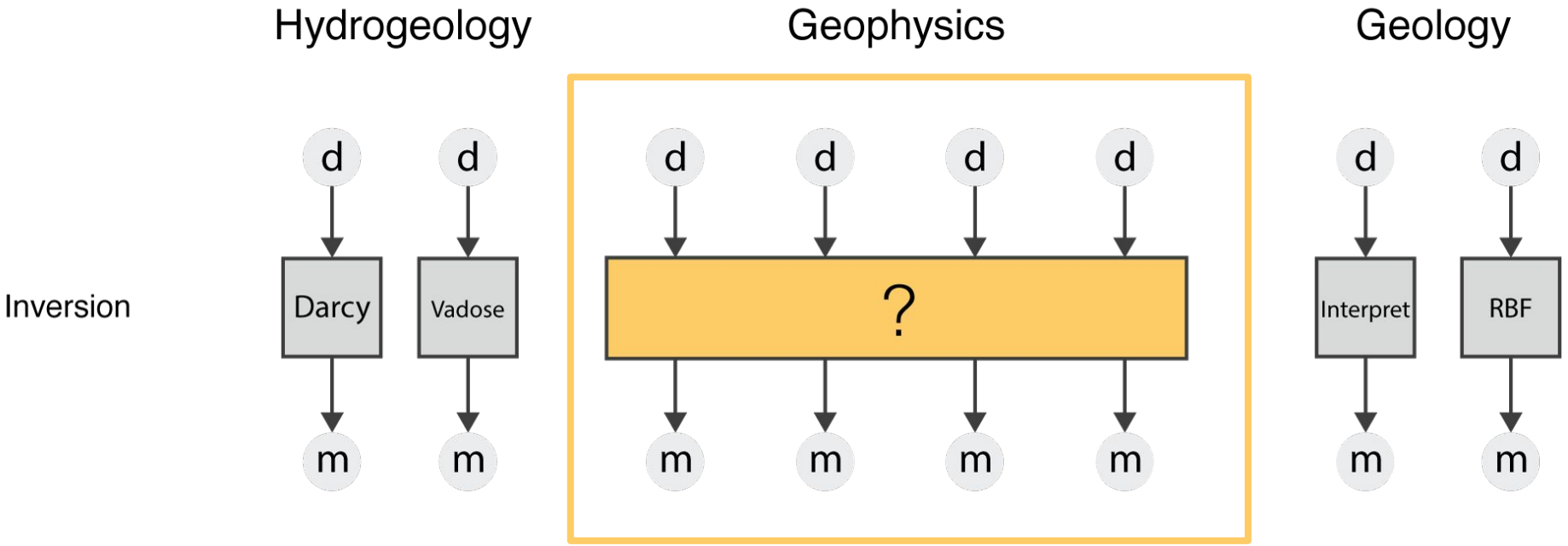
Hydrogeology
Geophysics
Geology
Inversion
d
d
d
d
d
d
d
Darcy
Vadose
?
Interpret
RBF
m
m
m
m
m
m
m

Inversion

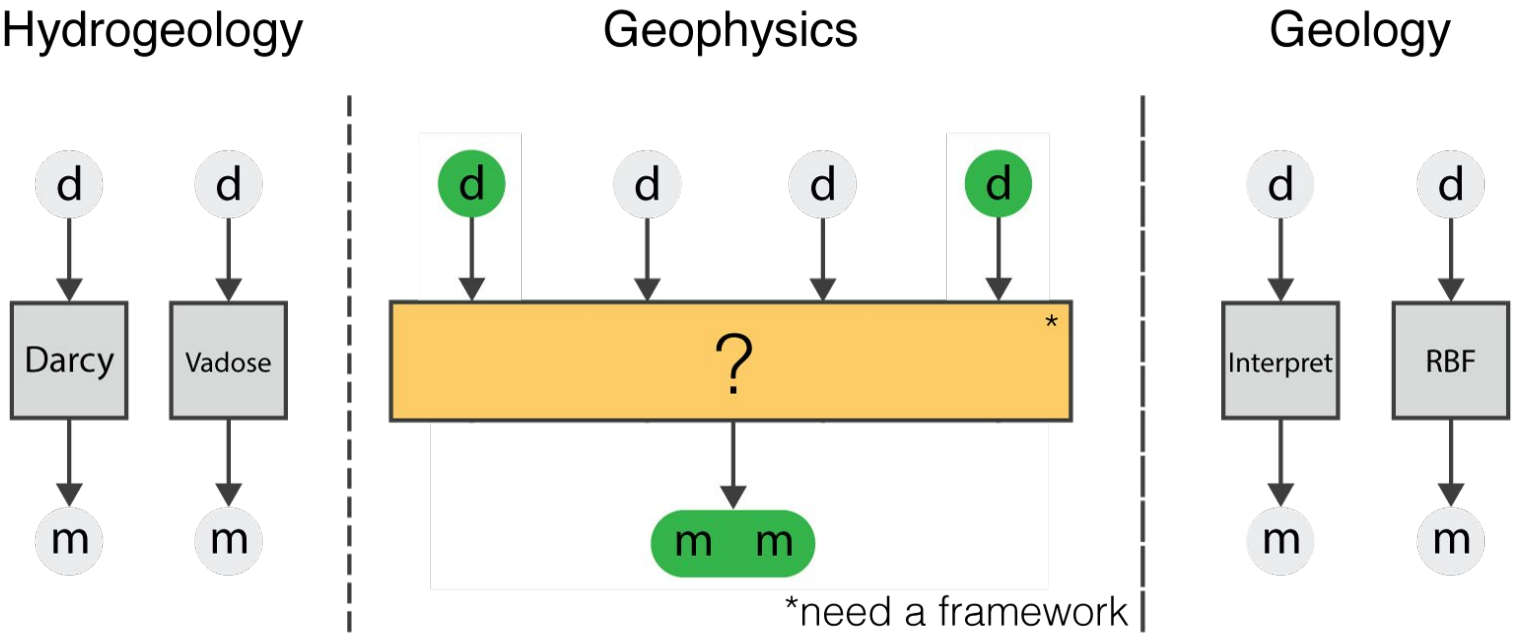
Hydrogeology
Geophysics
Geology
d
d
Darcy
Vadose
m
m
d
d
d
d
?
*
m
m
*need a framework
d
d
Interpret
RBF
m
m

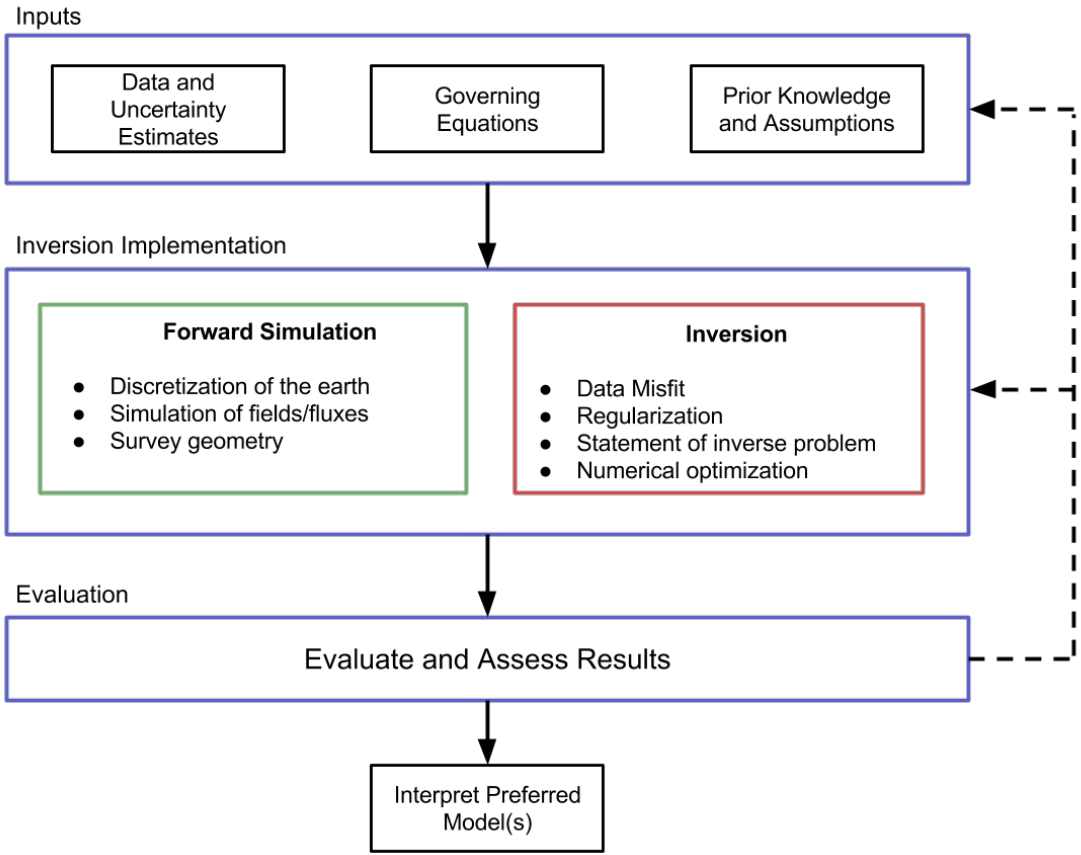
Inputs
Data and Uncertainty Estimates
Governing Equations
Prior Knowledge and Assumptions
Inversion Implementation
Forward Simulation
Discretization of the earth
Simulation of fields/fluxes
Survey geometry
Inversion
Data Misfit
Regularization
Statement of inverse problem
Numerical optimization
Evaluation
Evaluate and Assess Results
Interpret Preferred Model(s)

Science! (in SimPEG)

Data
- Tx
- Rx
- Freq/times
- type ($E_x$, $E_y$, ...)
- dobs
- projectFields(u=None)
- setProblems
- dpred(m)
- residual
- residualWeighted
- plotData → predictSensitivities
- filter → only some data → stochastic
- survData
- covData: std*eps + floor

Mesh
- h / H / refine
- x0
- operators

Model
- eg. byCondModel
- m [array?]
- transforms ..
- transformDeriv ..

Problem
- mesh
- J (-approx)
- Jt (-approx)
- J dense
- createSyntheticData → doEndIteration
- u ← fields • Data needed for Tx locs.
- diagJtJ (-approx)
- traceJtJ (-approx)

Inversion Reg Optimization. ObjFunc
- *functions
  - → β
  - → mref
  - → reg
  - → obj funct.
  - → Model

$m_n = H^{-1} g$

$J \delta m = \delta d$

$\| J \delta m - \delta d \|^2$

$\delta m = (J^T J_i)^{-1} J^T \delta d$

Mesh → Problem, Model (Reg)
Problem → data
data, Model (Reg) → ObjFunction
ObjFunction, Optimization → Inversion

*
- How do we explain the data?
- What problem explains this data?
- How do we optimize a model to fit this data?

We create models and physics that explain data!

```
In [1]: import SimPEG

In [ ]: SimPEG.
```

- SimPEG.DataMisfit
- SimPEG.Directives
- SimPEG.InvProblem
- SimPEG.Inversion
- SimPEG.Maps
- SimPEG.Mesh
- SimPEG.Models
- SimPEG.Optimization
- SimPEG.Problem
- SimPEG.Regularization

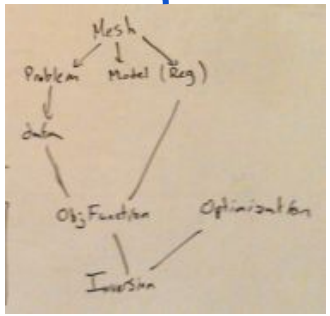


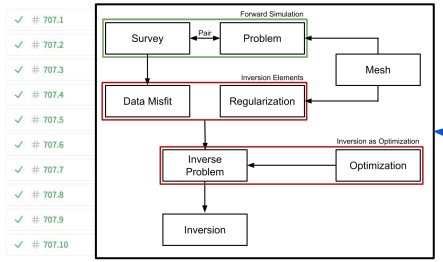


✓ # 707.1
✓ # 707.2
✓ # 707.3
✓ # 707.4
✓ # 707.5
✓ # 707.6
✓ # 707.7
✓ # 707.8
✓ # 707.9
✓ # 707.10

```
test_rotatePointsFromNormals (tests.utils.test_coordutils.coorUtilsTest) ... ok
test_rotationMatrixFromNormals (tests.utils.test_coordutils.coorUtilsTest) ... ok
test_simpleFail (tests.utils.test_utils.TestCheckDerivative) ... ok
test_simpleFunction (tests.utils.test_utils.TestCheckDerivative) ... ok
test_simplePass (tests.utils.test_utils.TestCheckDerivative) ... ok
test_simpleFail (tests.utils.test_utils.TestCounter) ... ok
testOnes (tests.utils.test_utils.TestDiagEst) ... ok
test_TensorType2D (tests.utils.test_utils.TestSequenceFunctions) ... ok
test_TensorType3D (tests.utils.test_utils.TestSequenceFunctions) ... ok
test_asArray_N_x_Dim (tests.utils.test_utils.TestSequenceFunctions) ... ok
test_ind2sub (tests.utils.test_utils.TestSequenceFunctions) ... ok
test_indexCube_2D (tests.utils.test_utils.TestSequenceFunctions) ... ok
test_indexCube_3D (tests.utils.test_utils.TestSequenceFunctions) ... ok
test_invPropertyTensor2D (tests.utils.test_utils.TestSequenceFunctions) ... ok
test_invPropertyTensor3D (tests.utils.test_utils.TestSequenceFunctions) ... ok
test_invXXXBlockDiagonal (tests.utils.test_utils.TestSequenceFunctions) ... ok
test_isScalar (tests.utils.test_utils.TestSequenceFunctions) ... ok
test_mkvc1 (tests.utils.test_utils.TestSequenceFunctions) ... ok
test_mkvc2 (tests.utils.test_utils.TestSequenceFunctions) ... ok
test_mkvc3 (tests.utils.test_utils.TestSequenceFunctions) ... ok
test_ndgrid_2D (tests.utils.test_utils.TestSequenceFunctions) ... ok
test_ndgrid_3D (tests.utils.test_utils.TestSequenceFunctions) ... ok
test_sub2ind (tests.utils.test_utils.TestSequenceFunctions) ... ok

----------------------------------------------------------------------
Ran 430 tests in 245.984s

OK
```

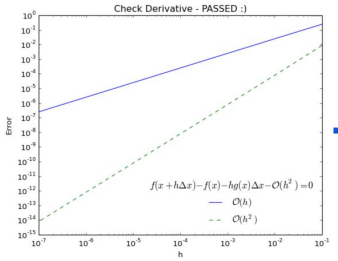


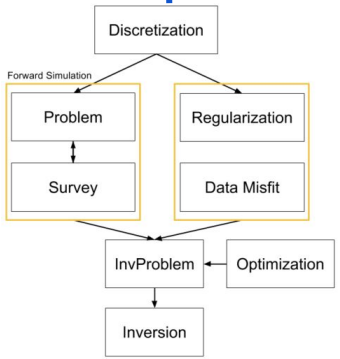

# Implementation

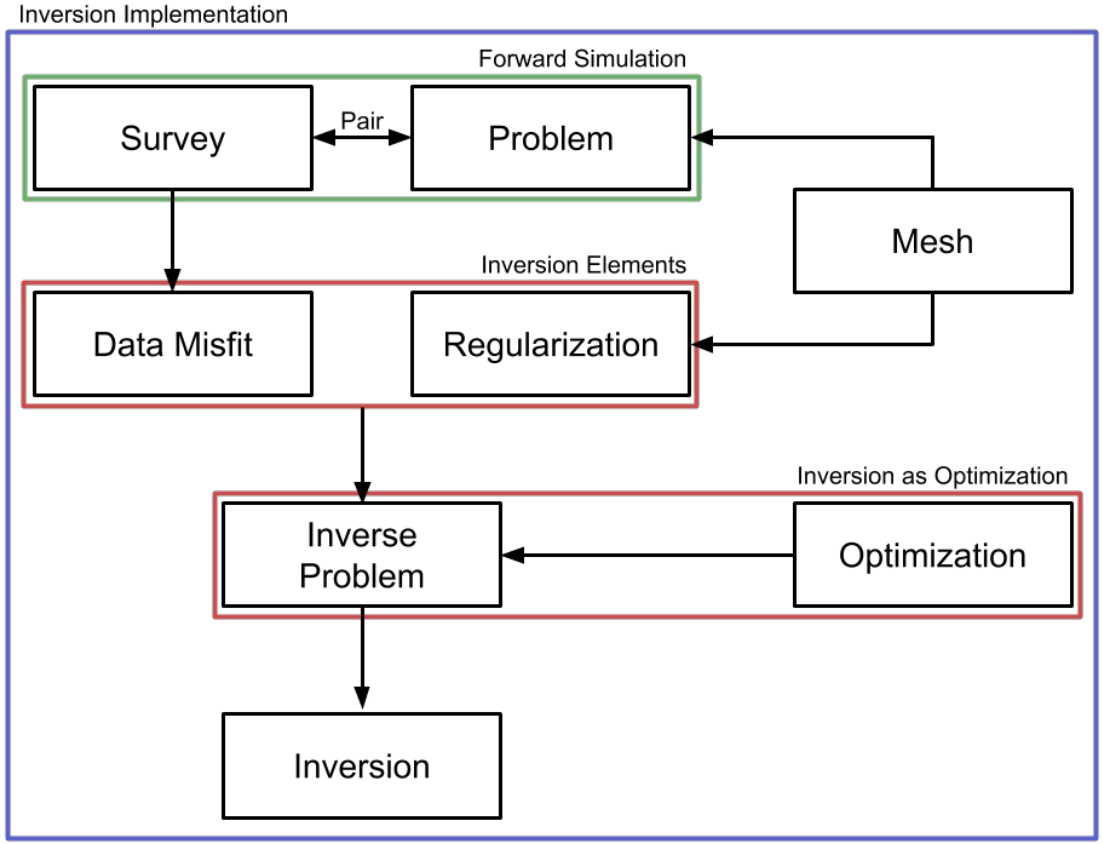

# Interactive Geophysics!

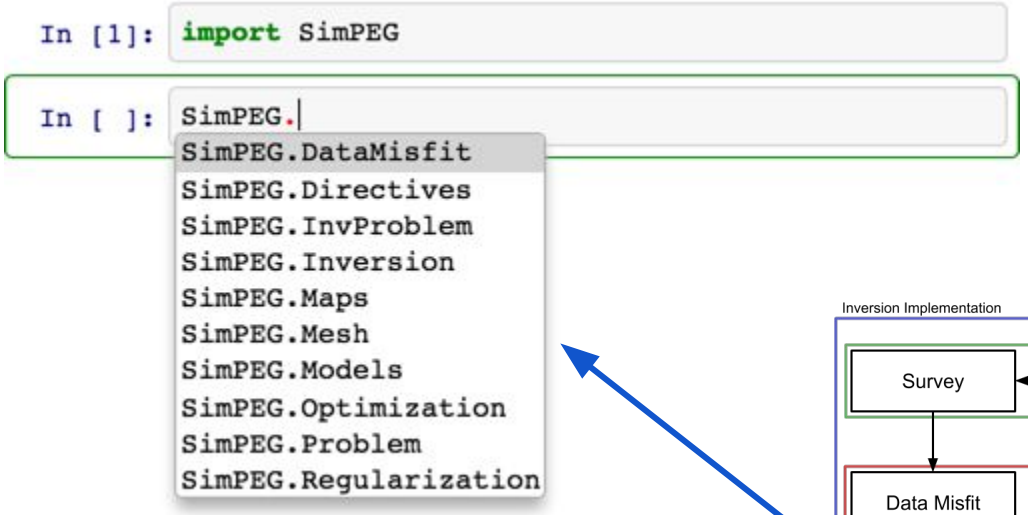


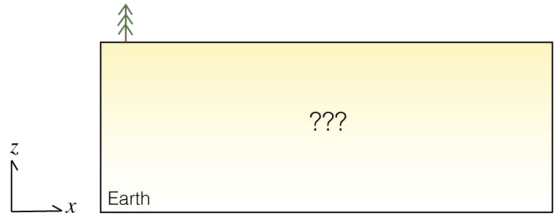


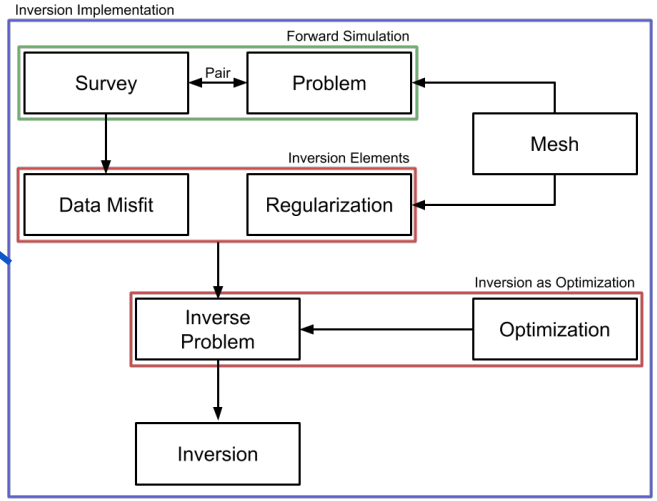

# Survey & Problem

Data collection and geometry

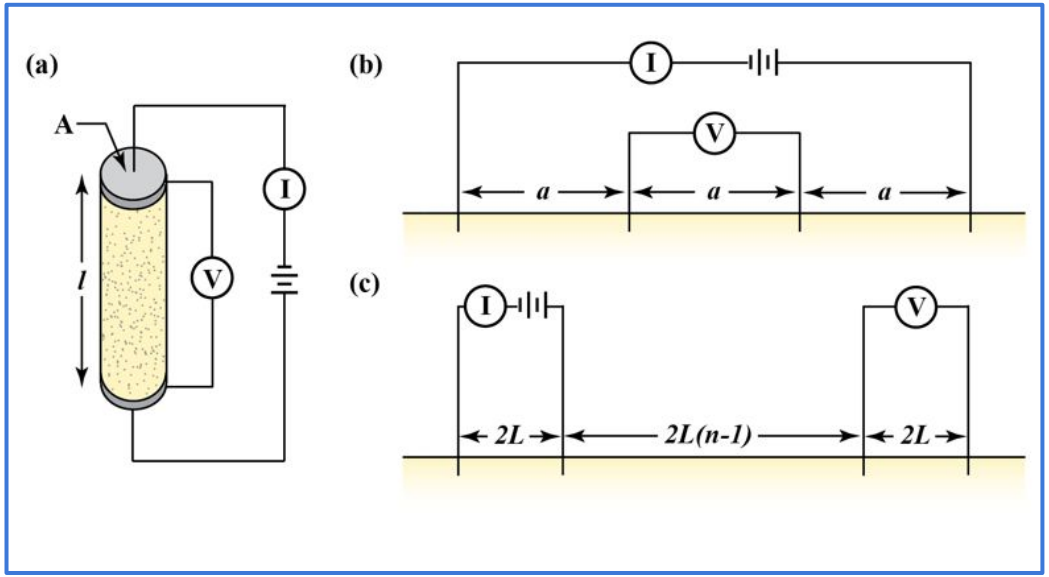


Physics

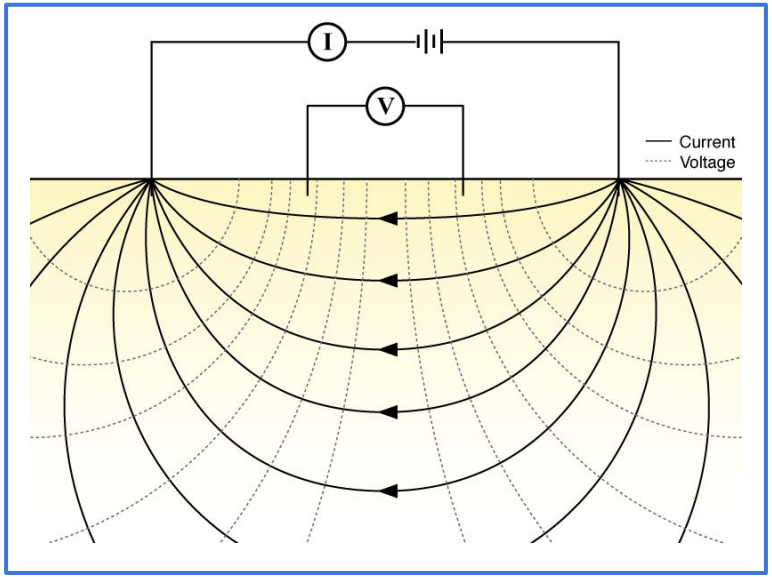

# Finite Volume

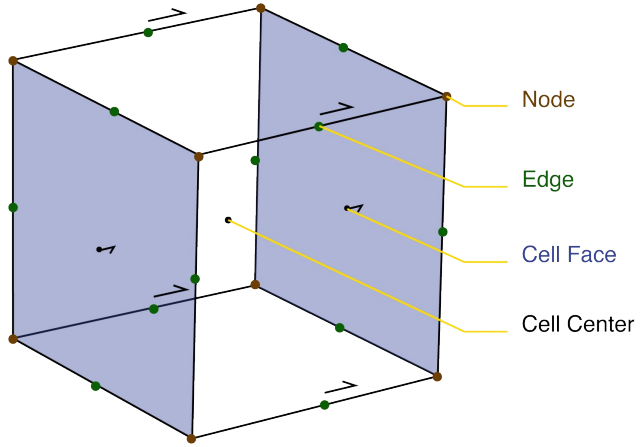


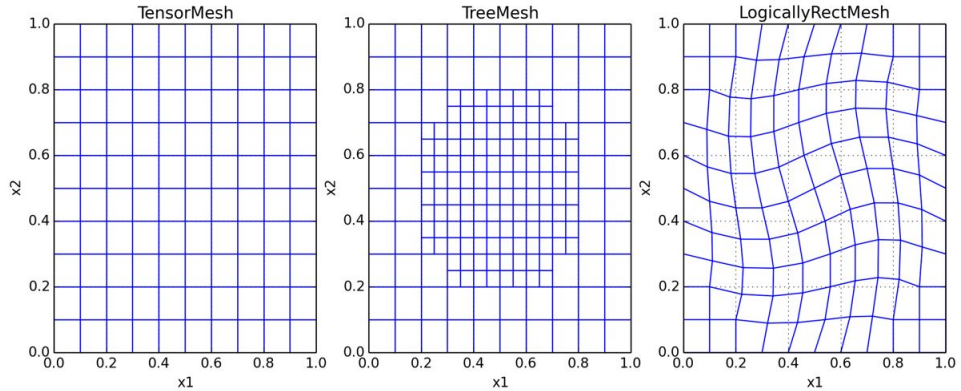


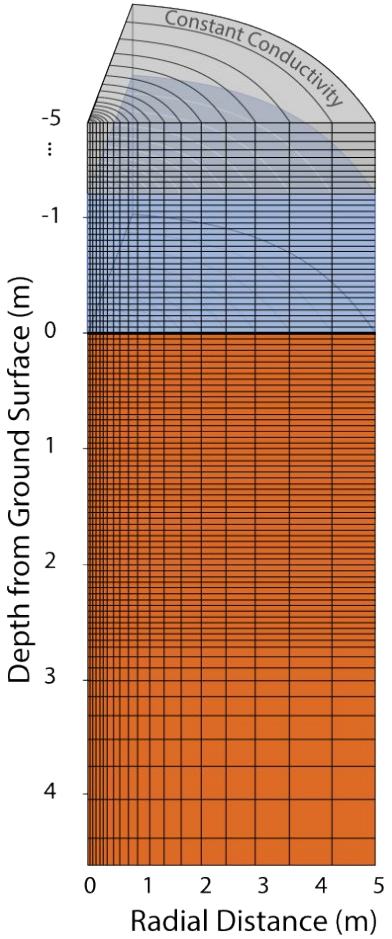

# Creating a Mesh

```
hx = [3,2,1,1,1,1,2,3]
hy = [3,1,1,3]
M = Mesh.TensorMesh([hx, hy])
M.plotGrid(faces=True, nodes=True, centers=True)
```

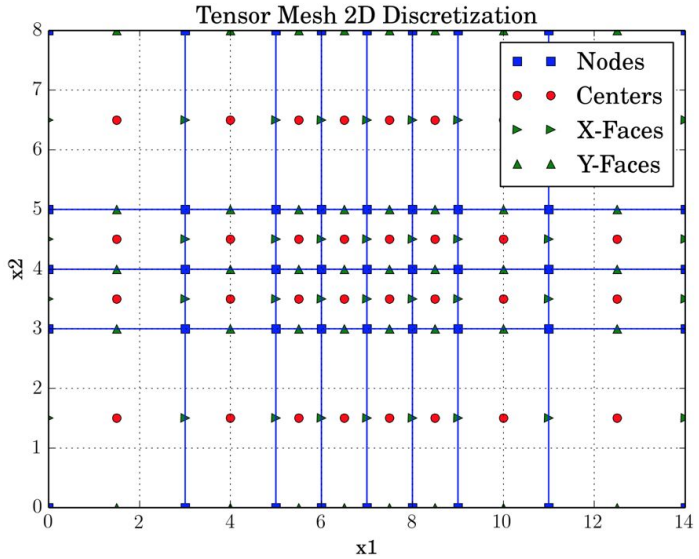


| Property or Function |
|---|
| dim, x0 |
| nC, nN, nF, nE |
| vol, area, edge |
| gridN, gridCC, ... |
| faceDiv, edgeCurl, cellGrad |
| aveF2CC, aveN2CC, etc. |
| getEdgeInnerProduct() |
| getInterpolationMat(loc) |

# DC Resistivity

$$\nabla \cdot (-\sigma \nabla \phi) = \mathbf{I}(\delta(\mathbf{r} - \mathbf{r_{s^+}}) - \delta(\mathbf{r} - \mathbf{r_{s^-}}))$$

```
D = M.faceDiv
G = M.cellGrad
# Harmonically average sigma
MsigI = sdInv(sdiag(M.aveF2CC.T*(1/sig)))
A = D*MsigI*G
A[0,0] *= 1/M.vol[0] # Remove the null space
Ainv = Solver(A) # Create a default Solver
phi = Ainv * ( - q )
```

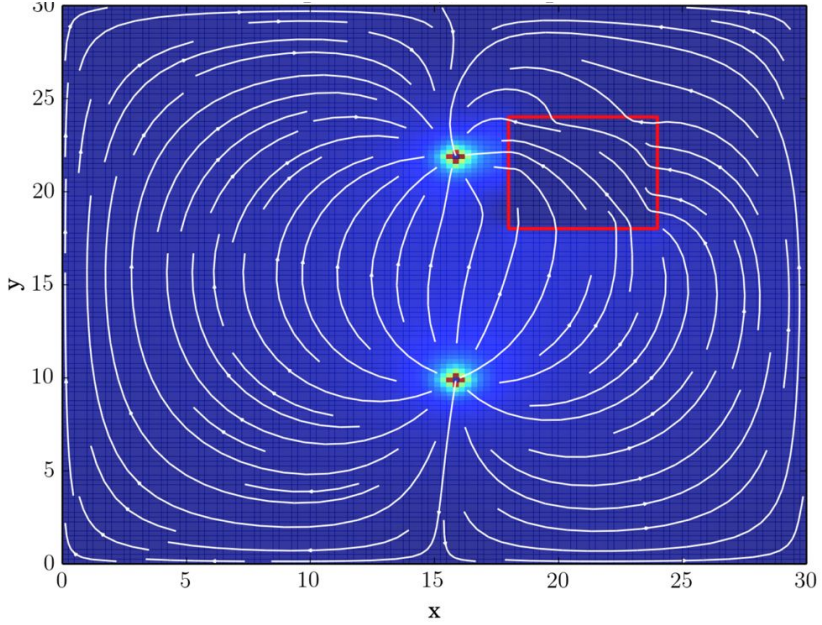

# DC Resistivity

$$\nabla \cdot (-\sigma \nabla \phi) = \mathbf{I}(\delta(\mathbf{r} - \mathbf{r_{s^+}}) - \delta(\mathbf{r} - \mathbf{r_{s^-}}))$$

```
D = M.faceDiv
G = M.cellGrad
# Harmonically average sigma
MsigI = sdInv(sdiag(M.aveF2CC.T*(1/sig)))
A = D*MsigI*G
A[0,0] *= 1/M.vol[0] # Remove the null space
Ainv = Solver(A) # Create a default Solver
phi = Ainv * ( - q )
```

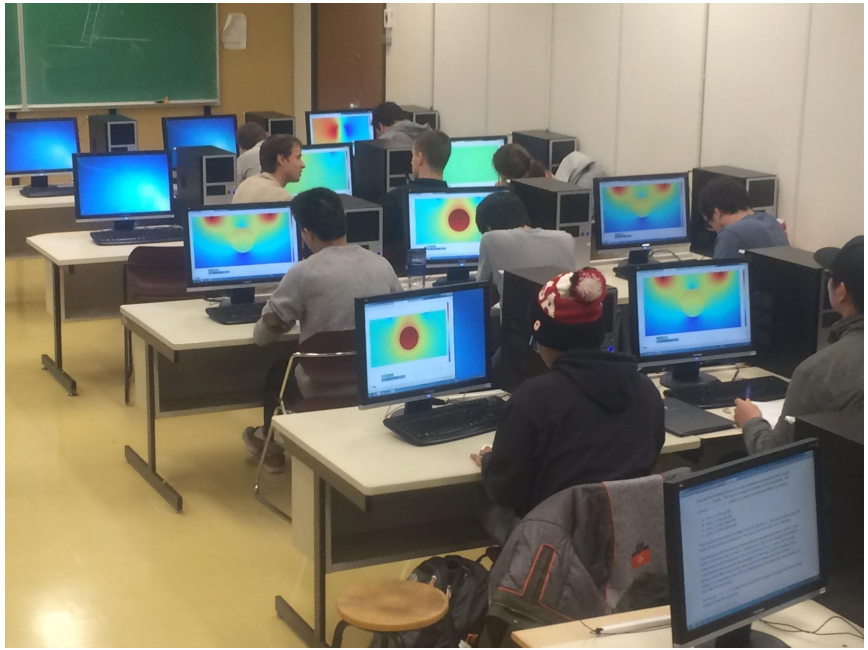

# Time Domain Electromagnetics

32 lines of code

$$\nabla \times \vec{e} + \frac{\partial \vec{b}}{\partial t} = 0,$$

$$\nabla \times \frac{1}{\mu_0}\vec{b} - \sigma \vec{e} = \vec{j}_s.$$

$$\mathbf{C}\vec{e}^{(t+1)} + \frac{\vec{b}^{(t+1)} - \vec{b}^{(t)}}{\Delta t} = 0$$

$$\mathbf{C}^\top \mathbf{M}^f_{\mu^{-1}} \vec{b}^{(t+1)} - \mathbf{M}^e_\sigma \vec{e}^{(t+1)} = \mathbf{M}^e \vec{j}_s^{(t+1)}$$

```python
from SimPEG import *
import simpegEM as EM
from pymatsolver import MumpsSolver
from scipy.constants import mu_0

# Create the computational mesh
cs, nc, npad = 20., 20, 5 # cell sz, num cells/padding
h = [(cs,npad,-1.3),(cs,nc),(cs,npad,1.3)]
mesh = Mesh.TensorMesh([h,h,h], 'CCC')
# Create a half-space conductivity
sigma = np.ones(mesh.nC)*1e-8
sigma[mesh.gridCC[:,2] < 0] = 1e-3

# Create a source in the center of our domain (0,0,0)
As = EM.Sources.MagneticDipoleVectorPotential(
        np.zeros(3), mesh, ['Ex','Ey','Ez'])
C = mesh.edgeCurl
b0 = C*As

# Create inner products
MesigI = mesh.getEdgeInnerProduct(sigma, invMat=True)
Mfmui  = mesh.getFaceInnerProduct(1./mu_0)
Me     = mesh.getEdgeInnerProduct()

# Maxwell's Equation (eliminate e, j_s=0)
dt = 1e-7 # Choose a time-step
A = Mfmui*C*MesigI*C.T*Mfmui + 1.0/dt*Mfmui
Ainv = MumpsSolver(A) # Factor the matrix!
# Solve for b using Backward Euler!
B = [b0] + range(299)
for i in range(len(B)-1):
    B[i+1] = Ainv * ( 1.0/dt*Mfmui*B[i] )
```

# Implementation

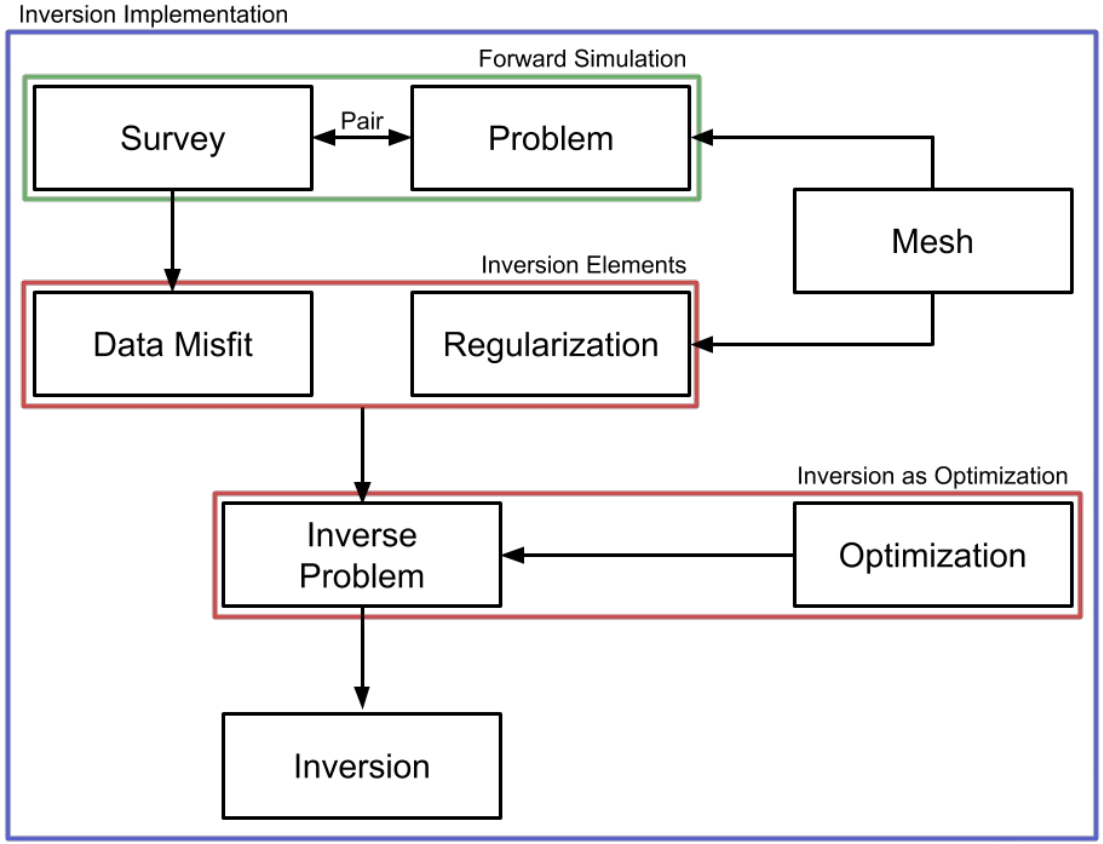

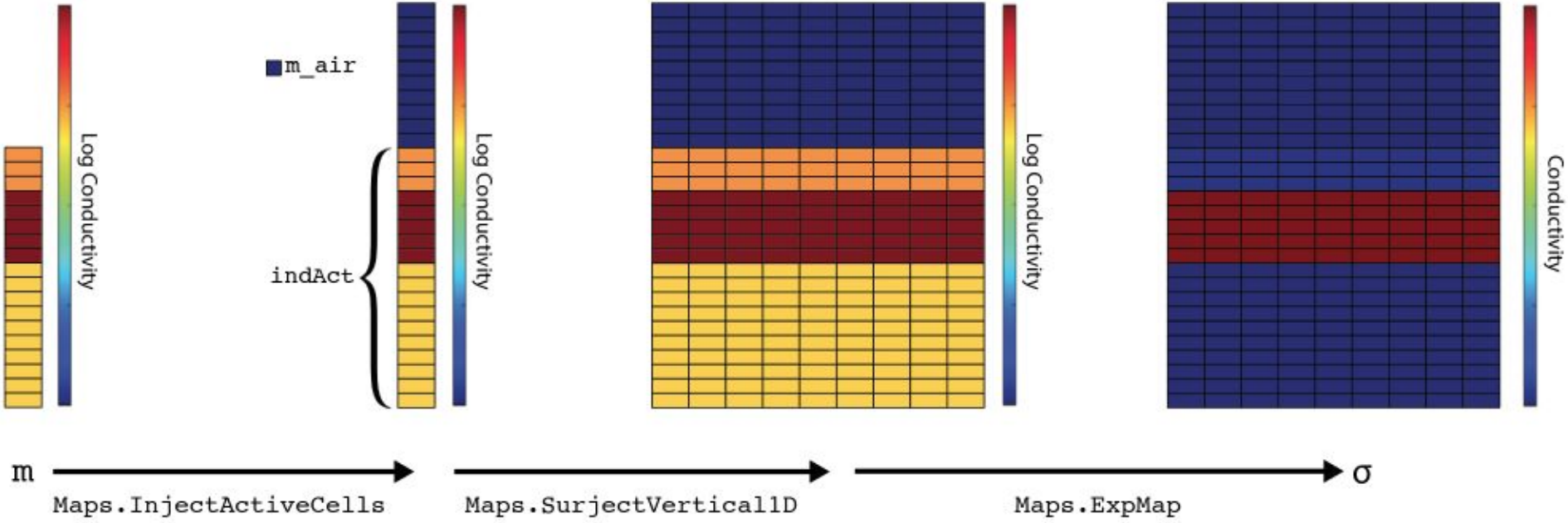


In [ ]:

```
from SimPEG import Mesh, Maps, np
mesh = Mesh.CylMesh([20, 20]) # SimPEG cylindrically symmetric mesh
m_air = np.log(1e-8) # value of the model in the air cells
indAct = mesh.vectorCCz < 0. # define active cells to be subsurface only
mapping = ( Maps.ExpMap(mesh) *
    Maps.SurjectVertical1D(mesh) *
    Maps.InjectActiveCells(mesh, indAct, m_air, nC=mesh.nCz) )
```

# Inversion Elements

Data Misfit

$$\phi_d(\mathbf{m}) = \frac{1}{2}\|\mathbf{W}_\mathrm{d}(F[\mathbf{m}] - \mathbf{d}_\mathrm{obs})\|_2^2$$

Regularization

$$\phi_m(\mathbf{m}) = \frac{1}{2}\|\mathbf{W}_\mathrm{m}(\mathbf{m} - \mathbf{m}_\mathrm{ref})\|_2^2$$

$$\phi(\mathbf{m}) = \phi_d(\mathbf{m}) + \beta\phi_m(\mathbf{m})$$

Inverse Problem

# Optimization

```
In [1]: from SimPEG import Optimization

In [ ]: Optimization.
```

```
Optimization.BFGS
Optimization.GaussNewton
Optimization.InexactGaussNewton
Optimization.IterationPrinters
Optimization.Minimize
Optimization.NewtonRoot
Optimization.ProjectedGNCG
Optimization.ProjectedGradient
Optimization.Remember
Optimization.Solver
```

$$\underset{\mathbf{m}}{\text{minimize}} \quad \phi(\mathbf{m}) = \phi_d(\mathbf{m}) + \beta\phi_m(\mathbf{m})$$

$$\text{s.t.} \quad \phi_d \leq \phi_d^*, \quad \mathbf{m}_i^L \leq \mathbf{m}_i \leq \mathbf{m}_i^H$$

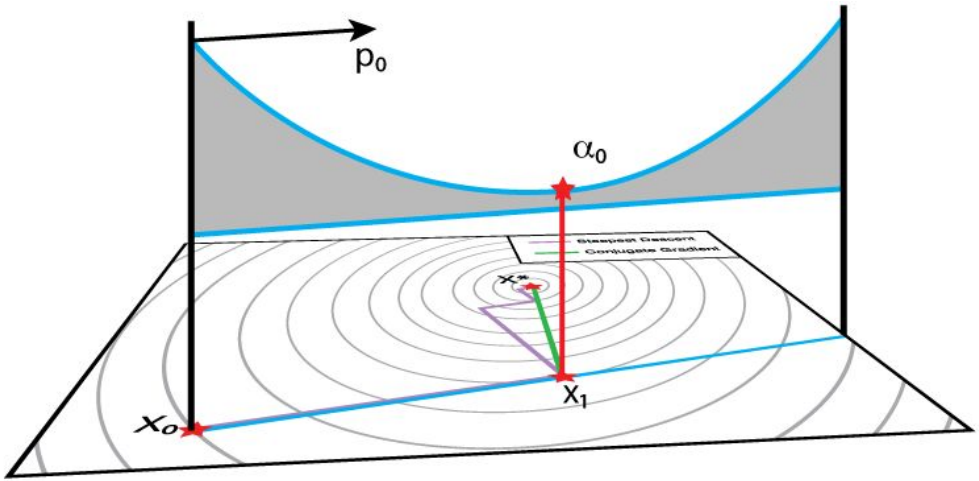

# Bringing it together.

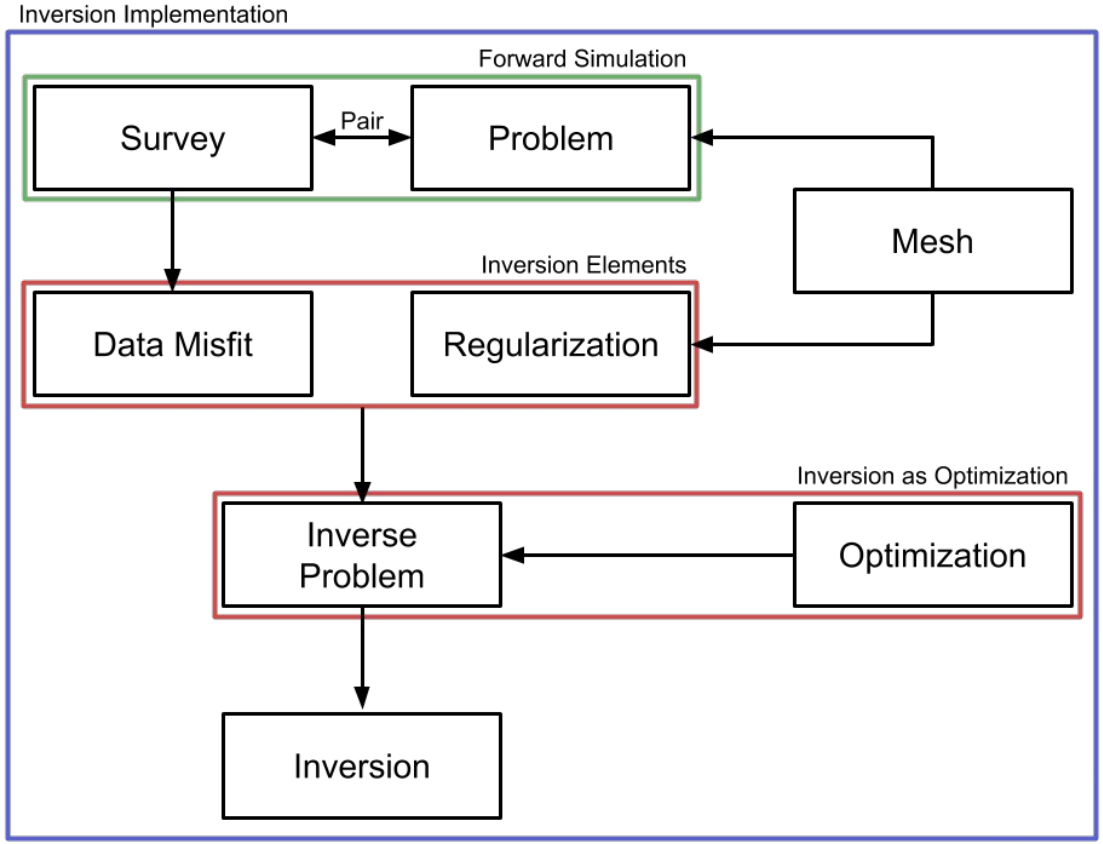

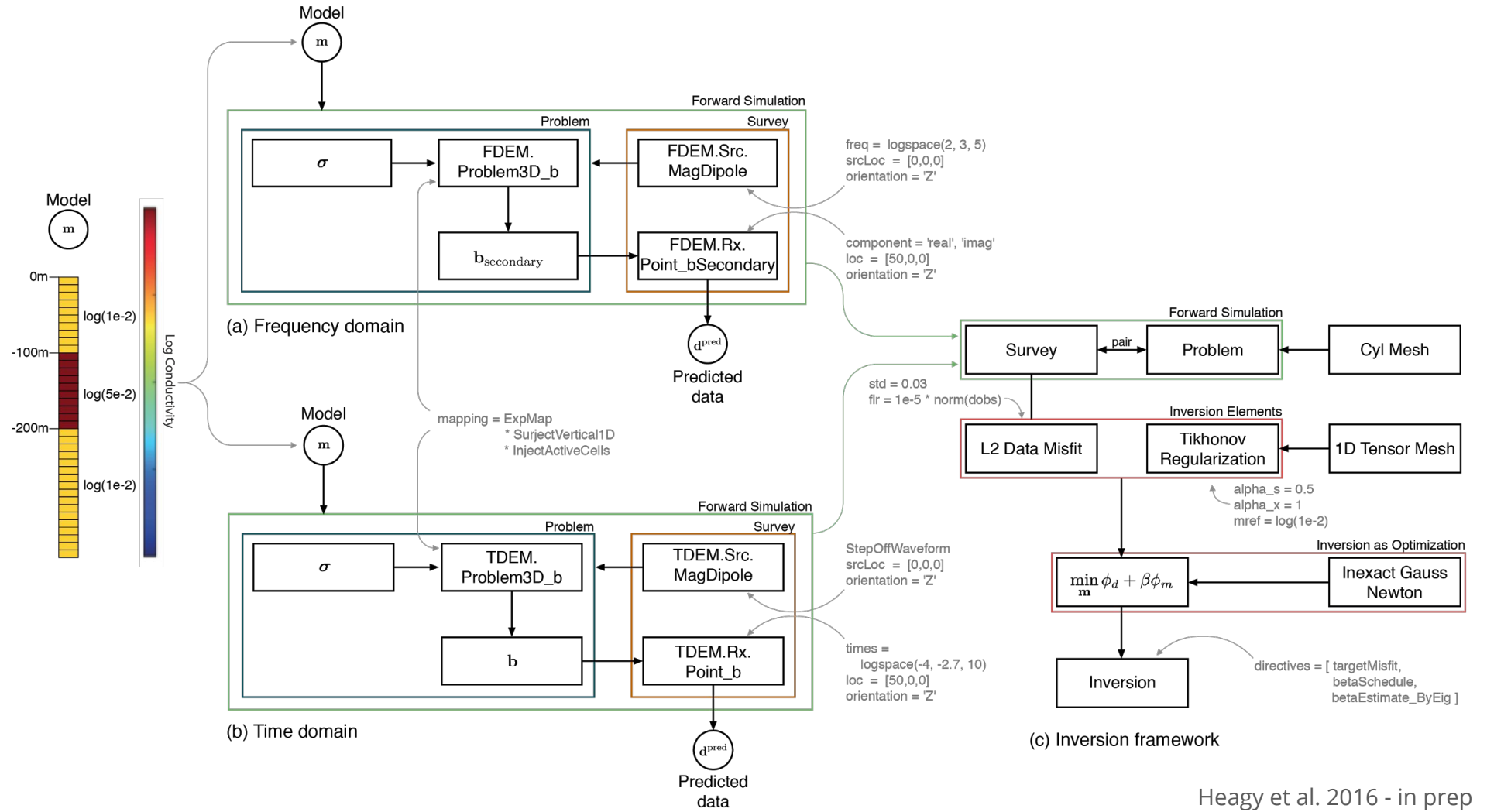


Heagy et al. 2016 - in prep

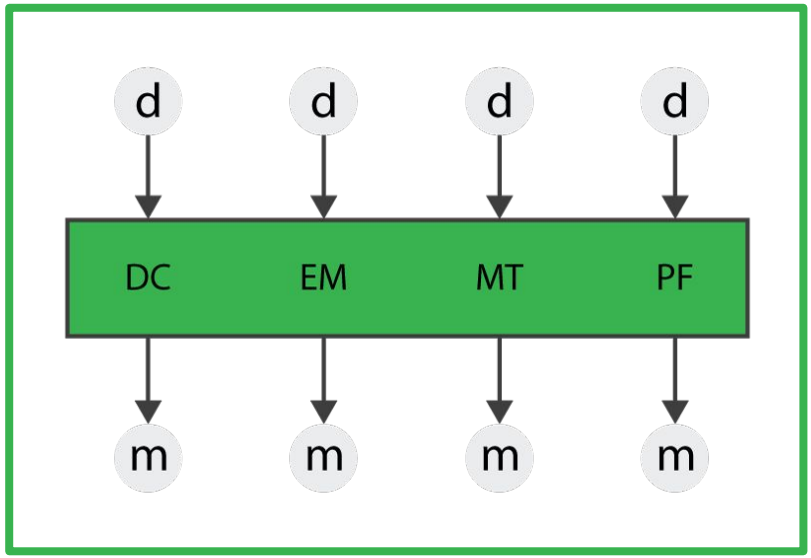
d
d
d
d
DC
EM
MT
PF
m
m
m
m

# Where are the diamonds?















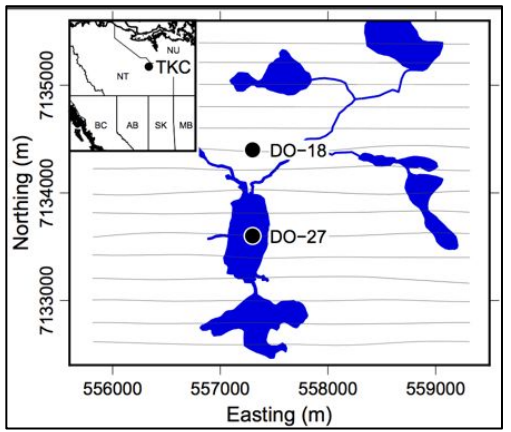


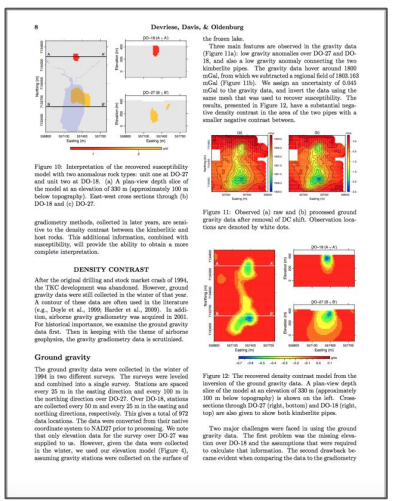

8 Devriese, Davis, & Oldenburg

Figure 10: Interpretation of the recovered susceptibility model with two anomalous rock types: unit one at DO-27 and unit two at DO-18. (a) A plan-view depth slice of the model at an elevation of 330 m (approximately 100 m below topography). East-west cross sections through (b) DO-18 and (c) DO-27.

gradiometry methods, collected in later years, are sensitive to the density contrast between the kimberlitic and host rocks. This additional information, combined with susceptibility, will provide the ability to obtain a more complete interpretation.

### DENSITY CONTRAST

After the original drilling and stock market crash of 1994, the TKC development was abandoned. However, ground gravity data were still collected in the winter of that year. A contour of these data are often used in the literature (e.g., Doyle et al., 1999; Harder et al., 2009). In addition, airborne gravity gradiometry was acquired in 2001. For historical importance, we examine the ground gravity data first. Then in keeping with the theme of airborne geophysics, the gravity gradiometry data is scrutinized.

### Ground gravity

The ground gravity data were collected in the winter of 1994 in two different surveys. The surveys were leveled and combined into a single survey. Stations are spaced every 35 m in the easting direction and every 100 m in the northing direction over DO-27. Over DO-18, stations are collected every 50 m and every 25 m in the easting and northing directions, respectively. This gives a total of 972 data locations. The data were converted from their native coordinate system to NAD27 prior to processing. We note that only elevation data for the survey over DO-27 was supplied to us. However, given the data were collected in the winter, we used our elevation model (Figure 4), assuming gravity stations were collected on the surface of the frozen lake.

Three main features are observed in the gravity data (Figure 11a): low gravity anomalies over DO-27 and DO-18, and also a low gravity anomaly connecting the two kimberlite pipes. The gravity data hover around 1800 mGal, from which we subtracted a regional field of 1803.163 mGal (Figure 11b). We assign an uncertainty of 0.045 mGal to the gravity data, and invert the data using the same mesh that was used to recover susceptibility. The results, presented in Figure 12, have a substantial negative density contrast in the area of the two pipes with a smaller negative contrast between.

Figure 11: Observed (a) raw and (b) processed ground gravity data after removal of DC shift. Observation locations are denoted by white dots.

Figure 12: The recovered density contrast model from the inversion of the ground gravity data. A plan-view depth slice of the model at an elevation of 330 m (approximately 100 m below topography) is shown on the left. Cross-sections through DO-27 (right, bottom) and DO-18 (right, top) are also given to show both kimberlite pipes.

Two major challenges were faced in using the ground gravity data. The first problem was the missing elevation over DO-18 and the assumptions that were required to calculate that information. The second drawback became evident when comparing the data to the gradiometry

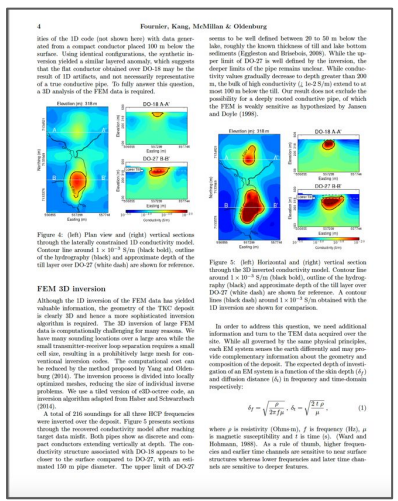

4 Fournier, Kang, McMillan & Oldenburg

ities of the 1D code (not shown here) with data generated from a compact conductor placed 100 m below the surface. Using identical configurations, the synthetic inversion yielded a similar layered anomaly, which suggests that the flat conductor obtained over DO-18 may be the result of 1D artifacts, and not necessarily representative of a true conductive pipe. To fully answer this question, a 3D analysis of the FEM data is required.

Figure 4: (left) Plan view and (right) vertical sections through the laterally constrained 1D conductivity model. Contour line around $1 \times 10^{-3}$ S/m (black bold), outline of the hydrography (black) and approximate depth of the till layer over DO-27 (white dash) are shown for reference.

### FEM 3D inversion

Although the 1D inversion of the FEM data has yielded valuable information, the geometry of the TKC deposit is clearly 3D and hence a more sophisticated inversion algorithm is required. The 3D inversion of large FEM data is computationally challenging for many reasons. We have many sounding locations over a large area while the small transmitter-receiver loop separation requires a small cell size, resulting in a prohibitively large mesh for conventional inversion codes. The computational cost can be reduced by the method proposed by Yang and Oldenburg (2014). The inversion process is divided into locally optimized meshes, reducing the size of individual inverse problems. We use a tiled version of cell-octree code, an inversion algorithm adapted from Haber and Schwarzbach (2014).

A total of 216 soundings for all three HCP frequencies were inverted over the deposit. Figure 5 presents sections through the recovered conductivity model after reaching target data misfit. Both pipes show as discrete and compact conductors extending vertically at depth. The conductivity structure associated with DO-18 appears to be closer to the surface compared to DO-27, with an estimated 150 m pipe diameter. The upper limit of DO-27 seems to be well defined between 20 to 50 m below the lake, roughly the known thickness of till and lake bottom sediments (Eggleston and Brisebois, 2008). While the upper limit of DO-27 is well defined by the inversion, the deeper limits of the pipe remains unclear. While conductivity values gradually decrease to depth greater than 200 m, the bulk of high conductivity ($\downarrow$ 1e-2 S/m) extend to at most 100 m below the till. Our result does not exclude the possibility for a deeply rooted conductive pipe, of which the FEM is weakly sensitive as hypothesized by Jansen and Doyle (1998).

Figure 5: (left) Horizontal and (right) vertical section through the 3D inverted conductivity model. Contour line around $1 \times 10^{-3}$ S/m (black bold), outline of the hydrography (black) and approximate depth of the till layer over DO-27 (white dash) are shown for reference. A contour lines (black dash) around $1 \times 10^{-3}$ S/m obtained with the 1D inversion are shown for comparison.

In order to address this question, we need additional information and turn to the TEM data acquired over the site. While all governed by the same physical principles, each EM system senses the earth differently and may provide complementary information about the geometry and composition of the deposit. The expected depth of investigation of an EM system is a function of the skin depth ($\delta_f$) and diffusion distance ($\delta_t$) in frequency and time-domain respectively:

$$\delta_f \sim \sqrt{\frac{\rho}{2\pi f \mu}}, \delta_t \sim \sqrt{\frac{2\,t\,\rho}{\mu}}, \qquad (1)$$

where $\rho$ is resistivity (Ohms-m), $f$ is frequency (Hz), $\mu$ is magnetic susceptibility and $t$ is time (s). (Ward and Hohmann, 1988). As a rule of thumb, higher frequencies and earlier time channels are sensitive to near surface structures whereas lower frequencies and later time channels are sensitive to deeper features.

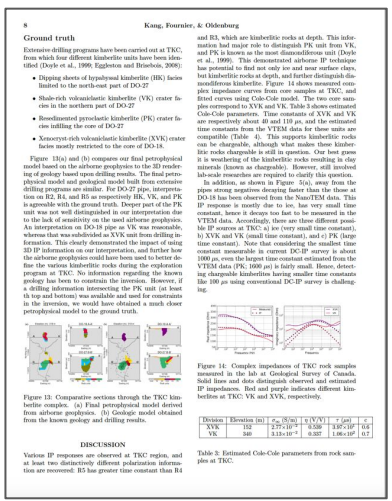

8 Kang, Fournier, & Oldenburg

### Ground truth

Extensive drilling programs have been carried out at TKC, from which four different kimberlite units have been identified (Doyle et al., 1999; Eggleston and Brisebois, 2008):

- Dipping sheets of hypabyssal kimberlite (HK) facies limited to the north-east part of DO-27
- Shale-rich volcaniclastic kimberlite (VK) crater facies in the northern part of DO-27
- Resedimented pyroclastic kimberlite (PK) crater facies infilling the core of DO-27
- Xenocryst-rich volcaniclastic kimberlite (XVK) crater facies mostly restricted to the core of DO-18.

Figure 13(a) and (b) compares our final petrophysical model based on the airborne geophysics to the 3D rendering of geology based upon drilling results. The final petrophysical model and geological model built from extensive drilling programs are similar. For DO-27 pipe, interpretation on R2, R4, and R5 as respectively HK, VK, and PK is agreeable with the ground truth. Deeper part of the PK unit was not well distinguished in our interpretation due to the lack of sensitivity on the used airborne geophysics. An interpretation on DO-18 pipe as VK was reasonable, whereas that was subdivided as XVK unit from drilling information. This clearly demonstrated the impact of using 3D IP information on our interpretation, and further how the airborne geophysics could have been used to better define the various kimberlitic rocks during the exploration program at TKC. No information regarding the known geology has been to constrain the inversion. However, if a drilling information intersecting the PK unit (at least th top and bottom) was available and used for constraints in the inversion, we would have obtained a much closer petrophysical model to the ground truth.

Figure 13: Comparative sections through the TKC kimberlite complex. (a) Final petrophysical model derived from airborne geophysics. (b) Geologic model obtained from the known geology and drilling results.

### DISCUSSION

Various IP responses are observed at TKC region, and at least two distinctively different polarization information are recovered: R5 has greater time constant than R4 and R3, which are kimberlitic rocks at depth. This information had major role to distinguish PK unit from VK, and PK is known as the most diamondiferous unit (Doyle et al., 1999). This demonstrated airborne IP technique has potential to find not only ice and near surface clays, but kimberlitic rocks at depth, and further distinguish diamondiferous kimberlite. Figure 14 shows measured complex impedance curves from core samples at TKC, and fitted curves using Cole-Cole model. The two core samples correspond to XVK and VK. Table 3 shows estimated Cole-Cole parameters. Time constants of XVK and VK are respectively about 40 and 110 $\mu$s, and the estimated time constants from the VTEM data for these units are compatible (Table 4). This supports kimberlitic rocks can be chargeable, although what makes these kimberlitic rocks chargeable is still in question. Our best guess it is weathering of the kimberlitic rocks resulting in clay minerals (known as chargeable). However, still involved lab-scale researches are required to clarify this question.

In addition, as shown in Figure 5(a), away from the pipes strong negatives decaying faster than the those at DO-18 has been observed from the NanoTEM data. This IP response is mostly due to ice, has very small time constant, hence it decays too fast to be measured in the VTEM data. Accordingly, there are three different possible IP sources at TKC: a) ice (very small time constant), b) XVK and VK (small time constant), and c) PK (large time constant). Note that considering the smallest time constant measurable in current DC-IP survey is about 1000 $\mu$s, even the largest time constant estimated from the VTEM data (PK; 1600 $\mu$s) is fairly small. Hence, detecting chargeable kimberlites having smaller time constants like 100 $\mu$s using conventional DC-IP survey is challenging.

Figure 14: Complex impedances of TKC rock samples measured in the lab at Geological Survey of Canada. Solid lines and dots distinguish observed and estimated IP impedances. Red and purple indicates different kimberlites at TKC: VK and XVK, respectively.

| Division | Elevation (m) | $\sigma_\infty$ (S/m) | $\eta$ (V/V) | $\tau$ ($\mu$s) | $c$ |
|---|---|---|---|---|---|
| XVK | 152 | $2.77\times10^{-2}$ | 0.536 | $3.97\times10^{1}$ | 0.6 |
| VK | 340 | $3.13\times10^{-2}$ | 0.337 | $1.06\times10^{2}$ | 0.7 |

Table 3: Estimated Cole-Cole parameters from rock samples at TKC.

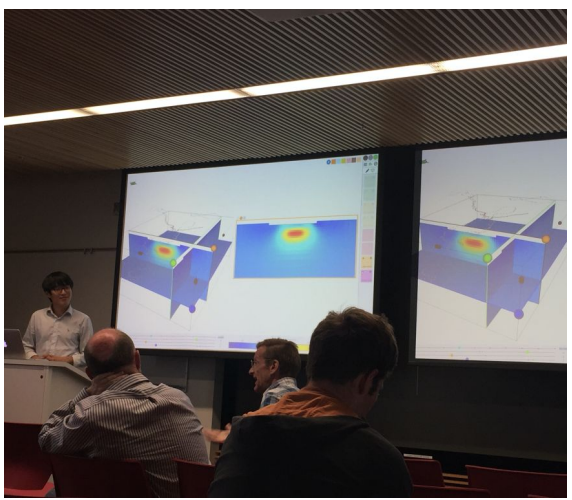

# Where are the diamonds?

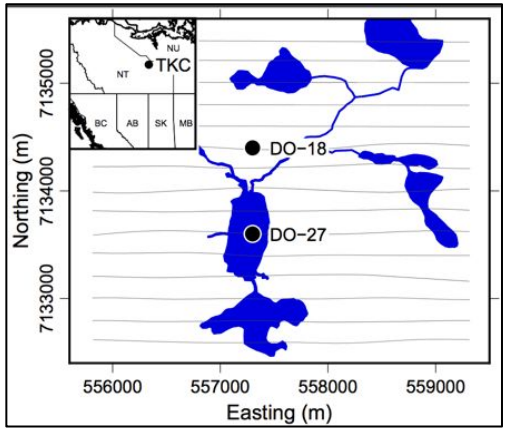


Kimberlite Pipe

- Different geologic units
- Specific units is diamond-rich

Physical Properties

- Low density
- Moderate susceptibility
- High conductivity

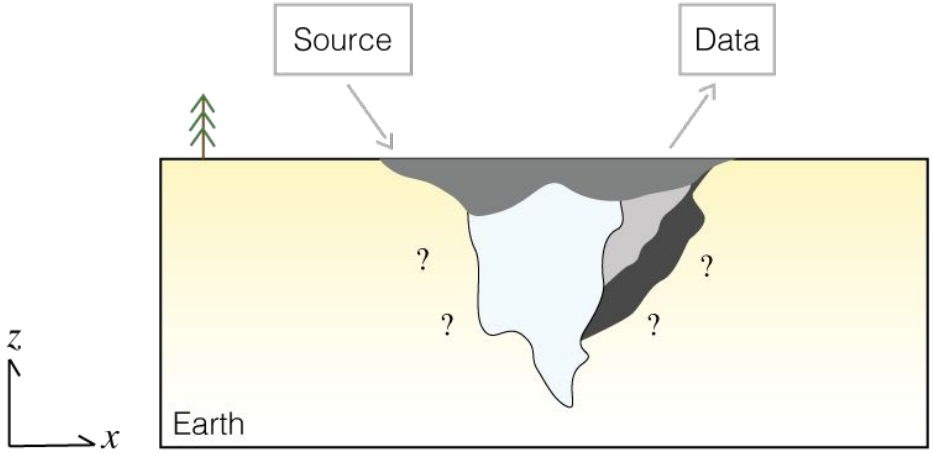

# Gravity

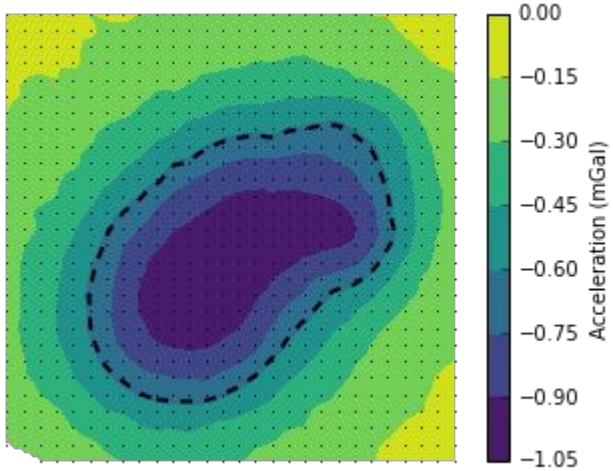


Rock model?

Recovered 3D Density

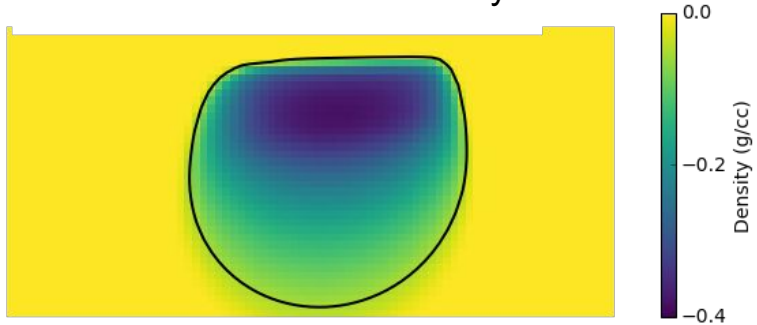


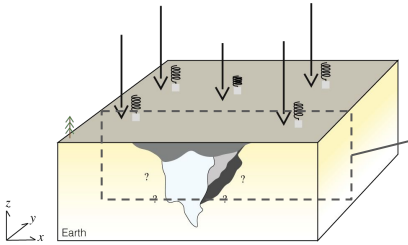


Vertical section

The world is 3D

# Magnetics

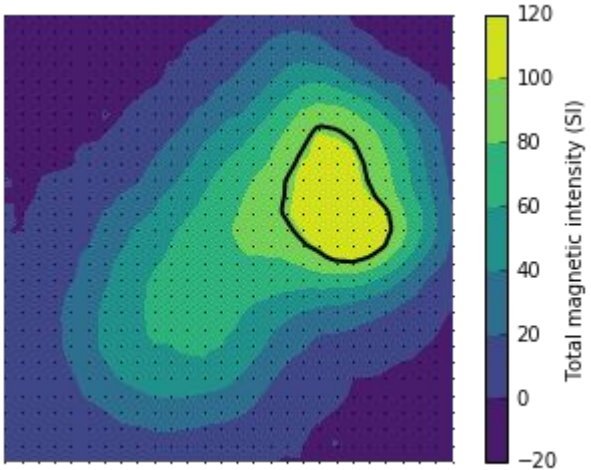


Rock model?

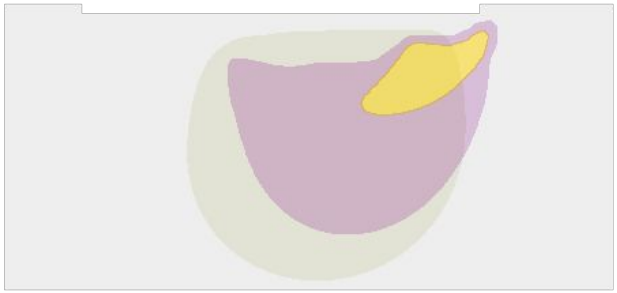

Recovered 3D Susceptibility

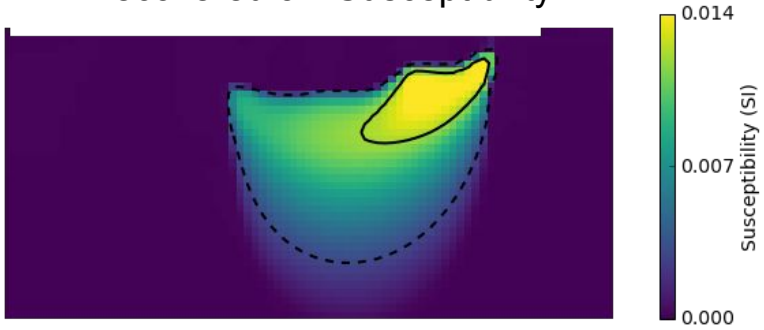


Vertical section

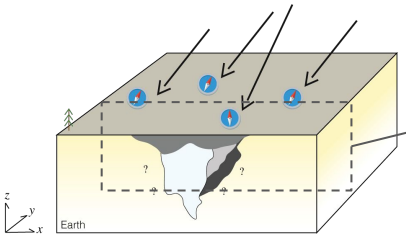


The world is 3D

# Direct Current (DC)

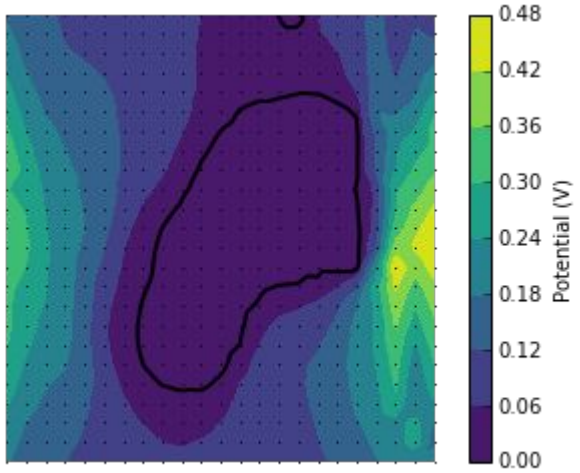


Rock model?

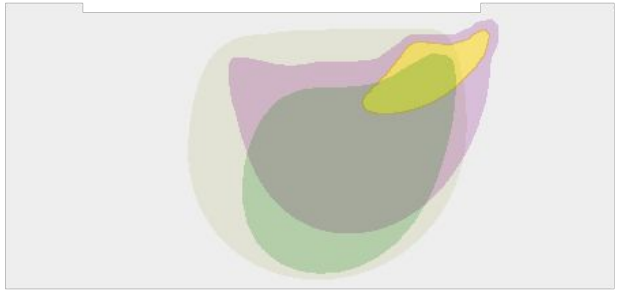

Recovered 3D Conductivity

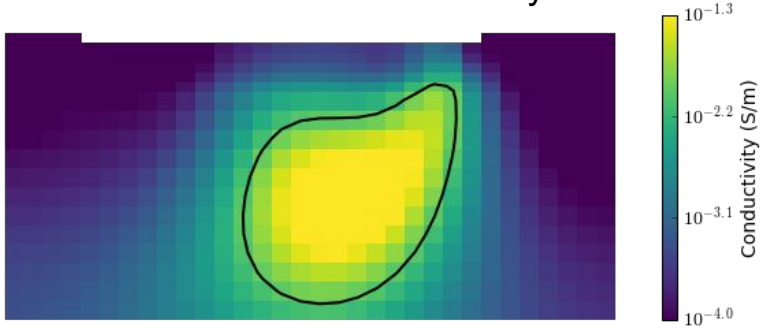


Vertical section

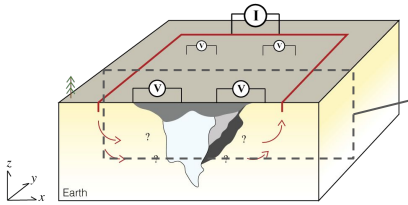


The world is 3D

# Magnetotellurics (MT)

1000 Hz

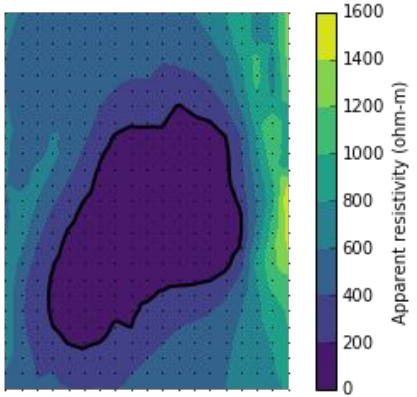


21544 Hz

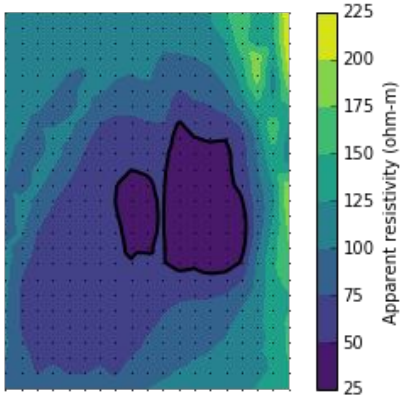


Rock model?

Recovered 3D Conductivity

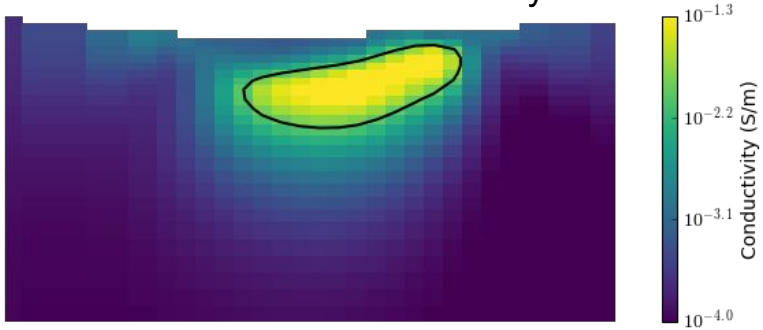


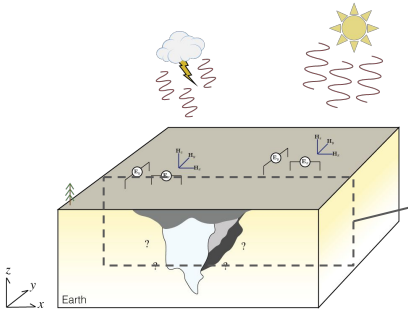


Vertical section

The world is 3D

# Integration or Interpretation?

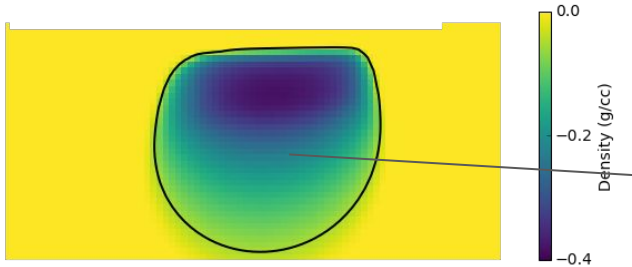


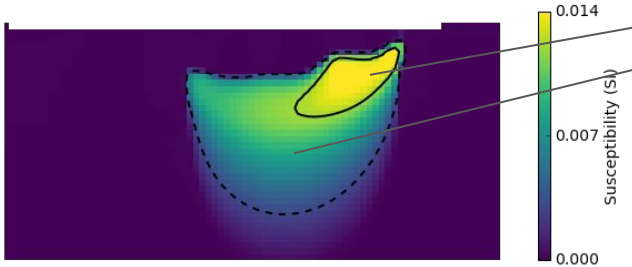


Rock model?

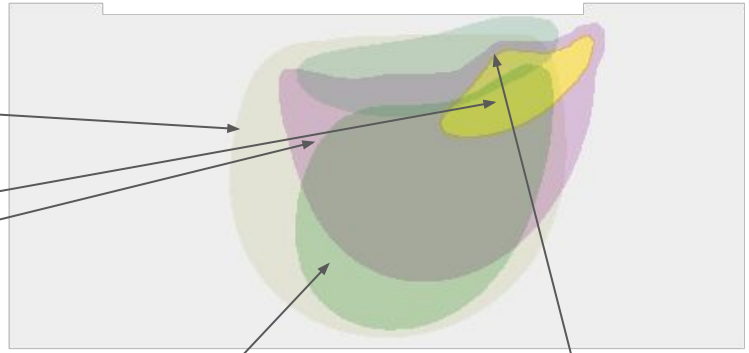

Diamond-rich kimberlite

- Low density
- Moderate susceptibility
- High conductivity

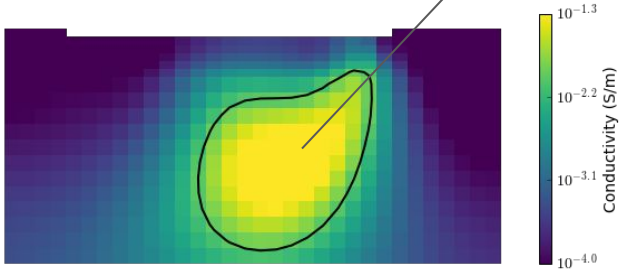


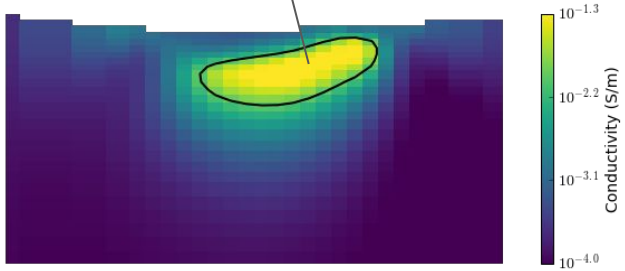

# Integration or Interpretation?

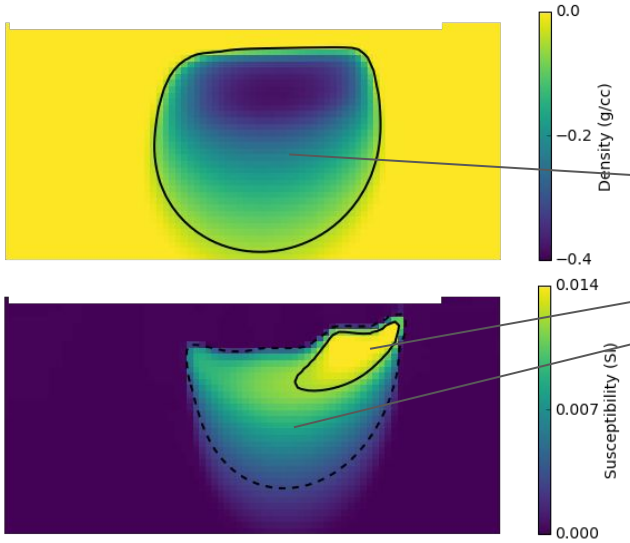


Rock model?

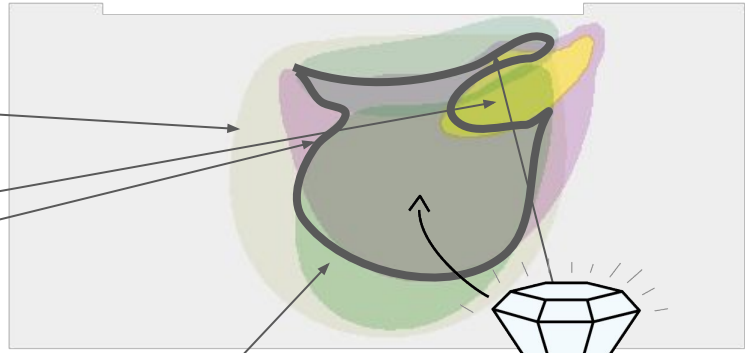



Diamonds?!

Diamond-rich kimberlite

- Low density
- Moderate susceptibility
- High conductivity

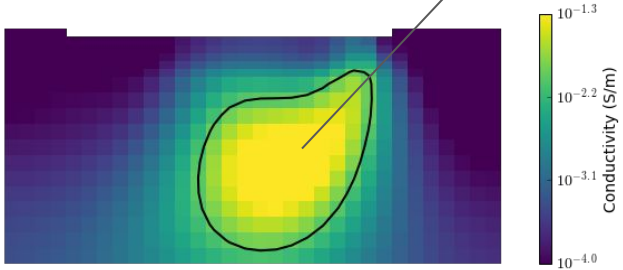


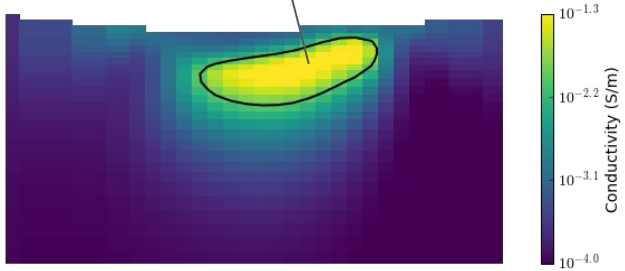

# From geophysics to a geologic model

Geologic model

Rock model from geophysics


http://simpeg.xyz